Channel Feedback Based on AoD-Adaptive Subspace Codebook in FDD Massive MIMO Systems

Wenqian Shen, Linglong Dai, Byonghyo Shim, Zhaocheng Wang, and Robert W. Heath, Jr.

***Abstract*— Channel feedback is essential in frequency division duplexing (FDD) massive multiple-input multiple-output (MIMO) systems. Unfortunately, prior work on multiuser MIMO has shown that the feedback overhead scales linearly with the number of base station (BS) antennas, which is large in massive MIMO systems. To reduce the feedback overhead, we propose an angle-of-departure (AoD) adaptive subspace codebook for channel feedback in FDD massive MIMO systems. Our key insight is to leverage the observation that path AoDs vary more slowly than the path gains. Within the angle coherence time, by utilizing the constant AoD information, the proposed AoD-adaptive subspace codebook is able to quantize the channel vector in a more accurate way. From the performance analysis, we show that the feedback overhead of the proposed codebook only scales linearly with a small number of dominant (path) AoDs instead of the large number of BS antennas. Moreover, we compare the proposed quantized feedback technique using the AoD-adaptive subspace codebook with a comparable analog feedback method. Extensive simulations show that the proposed AoD-adaptive subspace codebook achieves good channel feedback quality, while requiring low overhead.**

***Index Terms*— Massive MIMO, FDD, channel feedback, subspace codebook, AoD.**

I. Introduction

MASSIVE multiple-input multiple-output (MIMO) using hundreds of base station (BS) antennas is a key technology for 5G wireless communication systems. By simultaneously serving multiple users with simple linear precoders and combiners, massive MIMO can improve sum spectral efficiency by orders of magnitude [2]. Channel feedback is essential in frequency division duplex (FDD) massive MIMO systems to learn the channel state information at the transmitter (CSIT). Channel feedback techniques based on the pre-defined codebook known at both the BS and users have been widely used in wireless communication systems such as LTE/LTE-A, IEEE 802.11n/ac, and WiMAX [3]. Unfortunately, prior work on multiuser MIMO [4], [5] has shown that the feedback overhead scales linearly with the number of BS antennas to guarantee the capacity loss within an acceptable level. As the number of BS antennas in massive MIMO systems is much larger than that of current systems, the feedback overhead will be overwhelming.

A. Contributions

In this paper, we propose an angle-of-departure (AoD)-adaptive subspace codebook for massive MIMO channel feedback to reduce the feedback overhead.[1] Our main contributions are summarized as follows:

- We propose an AoD-adaptive subspace codebook with reduced feedback overhead. Specifically, we leverage the observation that path AoDs vary more slowly than path gains [6]. During a comparably long time called the "angle coherence time," which is different from the classical channel coherence time, the path AoDs can be regarded as unchanged, and known to both the BS and users. Within the angle coherence time, due to the limited scattering around the BS, the channel vector is distributed in the *channel subspace*, which is completely determined by a limited number of dominant path AoDs. By utilizing the AoD information, quantization vectors of the proposed AoD-adaptive subspace codebook are distributed exactly in the channel subspace. Therefore, quantized channel vector of the proposed codebook can achieve better performance.
- We provide performance analysis of the proposed AoD-adaptive subspace codebook in the large-dimension regime, i.e, the number of BS antennas grows large. Specifically, we first compute the per-user rate gap between the ideal case of the perfect CSIT and the

Manuscript received January 11, 2018; revised April 29, 2018; accepted June 6, 2018. Date of publication June 22, 2018; date of current version November 16, 2018. This work was supported by the National Natural Science Foundation of China for Outstanding Young Scholars (Grant No. 61722109), the National Research Foundation (Grant No. MSIP-2016R1A2B3015576), and the National Science Foundation (Grant No. ECCS-1711702, CNS-1702800, and CNS-1731658). This paper was presented in part at the IEEE International Conference on Communications, 2017 [1]. The associate editor coordinating the review of this paper and approving it for publication was D. B. da Costa. *(Corresponding author: Linglong Dai.)*

W. Shen is with the School of Information and Electronics, Beijing Institute of Technology, Beijing 100081, China (e-mail: wshen@bit.edu.cn).

L. Dai and Z. Wang are with the Department of Electronic Engineering, Tsinghua University, Beijing 100084, China (e-mail: daill@tsinghua.edu.cn; zcwang@tsinghua.edu.cn).

B. Shim is with the School of Electrical and Computer Engineering, Institute of New Media and Communications, Seoul National University, Seoul 151-742, South Korea (e-mail: bshim@snu.ac.kr).

R. W. Heath, Jr., is with the Department of Electrical and Computer Engineering, The University of Texas at Austin, Austin, TX 78712-1687 USA (e-mail: rheath@utexas.edu).

Color versions of one or more of the figures in this paper are available online at http://ieeexplore.ieee.org.

Digital Object Identifier 10.1109/TCOMM.2018.2849755

[1] Simulation codes are provided to reproduce the results presented in this paper: http://oa.ee.tsinghua.edu.cn/dailinglong/publications/publications.html.

practical case of the proposed quantized feedback technique using the AoD-adaptive subspace codebook. Our result reveals that such rate gap is dominated by the quantization error of channel vectors. Then, we derive an upper bound on the quantization error using the proposed AoD-adaptive subspace codebook. Finally, we show that the required number of feedback bits to ensure a constant rate gap only scales linearly with the number of dominant paths, which is much smaller than the number of BS antennas. Moreover, we compare the proposed quantized feedback technique using the AoD-adaptive subspace codebook with a comparable analog channel feedback method.

B. Prior Work

Several channel feedback techniques were proposed for massive MIMO systems. A compressive sensing (CS) based channel feedback scheme exploiting the sparsity of the angle-domain channel was proposed for massive MIMO systems in [7]. The channel vector is compressed into a low-dimension measurement vector by the random projection, and then fed back to the BS with low overhead. Then, the BS can recover the sparse angle-domain channel via CS algorithms. To further improve the channel recovery performance at the BS, the structured sparsity in the multiuser MIMO (MU-MIMO) channel matrix was exploited through a joint MU-MIMO channel recovery at the BS [8]. Distributed channel measurements of multiple users were fed back to the BS, and then the MU-MIMO channel matrix was recovered via a joint orthogonal matching pursuit algorithm. A non-uniform directional dictionary based channel feedback scheme was proposed with reduced feedback overhead by utilizing the directivity pattern of the angle-domain channel [9]. Other techniques were also developed for massive MIMO channel feedback using grouping techniques. An antenna grouping based channel feedback scheme was proposed in [10], where multiple correlated antennas were mapped to a single representative value using the predesigned mapping patterns. Therefore, the mapping pattern and the dimension-reduced channel vector after mapping can be fed back with reduced overhead. Joint spatial division and multiplexing (JSDM) proposed in [11] featured user grouping. Users with similar transmit channel covariance were grouped together. The inter-group interference was mitigated through a pre-precoding based on the known long-term channel statistics. After that, only the low-dimension intra-group channels were required to be fed back with low overhead to perform the MU-MIMO precoding for mitigating the intra-group interference.

There also exists some work on feedback codebook design. For example, a codebook was proposed in [12] under the framework of CS, which can quantize and feedback the low-dimension channel measurements with reduced overhead. Noncoherent trellis-coded quantization (NTCQ) was proposed in [13] by exploiting the duality between source encoding in a Grassmannian manifold and noncoherent sequence detection. The encoding complexity of NTCQ scales linearly with the number of BS antennas. Channel statistics were utilized for codebook design to reduce the feedback overhead [14]–[17]. In [14], a codebook was designed based on the assumption of line-of-sight (LOS) channels between users and the BS. It was shown that correlated fading in LOS channels is beneficial to MU-MIMO since it can significantly reduce the feedback overhead. A rotated codebook based on the channel statistics was proposed in [15] for the channel feedback of correlated channels composed of non-LOS channel paths. In that approach, it has been shown that the required number of feedback bits scales linearly with the rank of transmit channel correlation matrix [16], [17]. Our work is different from these channel statistics-based codebooks, as we exploit the concept of angle coherence time, so that the AoD information within the angle coherence time can be easily estimated with lower overhead, compared with the traditional channel statistics. The corresponding performance analysis of the proposed codebook is also different from previous work since our analysis is based on the AoD estimate, instead of the exact channel correlation matrix in traditional channel statistics-based codebook.

Besides, this paper differs from our previous work [1]. Specifically, we propose a channel subspace based analog feedback technique and compare it with the proposed quantized feedback technique using the AoD-adaptive subspace codebook. We also extend the AoD-adaptive subspace codebook to a more general scenario with a uniform planar array (UPA) of antennas at the BS. Moreover, we evaluate the effect of imperfect AoD information on the performance of the AoD-adaptive subspace codebook.

The rest of the paper is organized as follows. Section II presents the system model. In Section III, we firstly review the angle coherence time. Then, we present the proposed AoD-adaptive subspace codebook. Finally, we provide an AoD acquisition method. Performance analysis of the proposed AoD-adaptive subspace codebook is provided in Section IV. We propose a channel subspace based analog feedback technique and compare it with the proposed quantized feedback technique using the AoD-adaptive subspace codebook in Section V. Section VI shows the simulation results. Our conclusions are drawn in Section VII.

Notation: Boldface capital and lower-case letters stand for matrices and vectors, respectively. The transpose, conjugate, conjugate transpose, and inverse of a matrix are denoted by $(\cdot)^{\mathrm{T}}$, $(\cdot)^*$, $(\cdot)^{\mathrm{H}}$, and $(\cdot)^{-1}$, respectively. $\mathbf{H}^{\dagger} = \mathbf{H}(\mathbf{H}^{\mathrm{H}}\mathbf{H})^{-1}$ is the Moore-Penrose pseudo-inverse of $\mathbf{H}$. $\otimes$ is the Kronecker product operator. $\|\mathbf{h}\|$ and $|s|$ are the norm of a vector and the absolute value of a scalar. $\measuredangle(\mathbf{x}, \mathbf{y})$ is the angle between $\mathbf{x}$ and $\mathbf{y}$, and $\sin^2\left(\measuredangle\left(\mathbf{x}, \mathbf{y}\right)\right) = 1 - \frac{\left|\mathbf{x}^{\mathrm{H}}\mathbf{y}\right|^2}{\|\mathbf{x}\|^2\|\mathbf{y}\|^2}$. $\mathrm{E}\left[\cdot\right]$ denotes the expectation operator. Finally, $\mathbf{I}_P$ denotes the identity matrix of size $P \times P$.

II. Massive MIMO System Model

In this section, we introduce the massive MIMO downlink channel model and the quantized channel feedback technique. To quantify the performance of the feedback codebook, we review the per-user rate calculated assuming zero-forcing (ZF) precoding based on the feedback CSI.

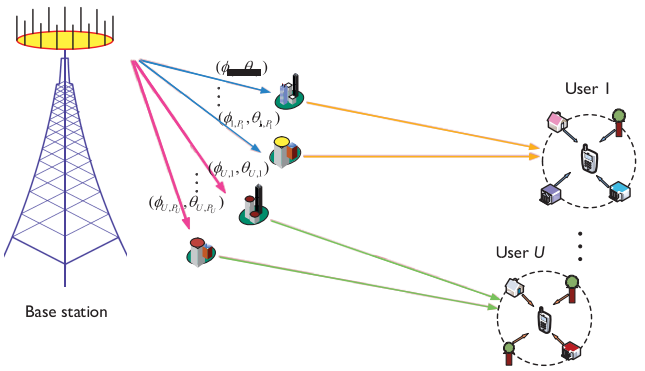

Fig. 1. Ray-based channel model, where the channel between the BS and the u-th user is composed of P_u dominant paths, each of which is characterized by a path gain $g_{u,i}$ and a path AoD $(\phi_{u,i}, \theta_{u,i})$.

A. Massive MIMO Downlink Channel Model

In this paper, we consider a massive MIMO system with M antennas at the BS and U single-antenna users ($M \gg U$) [2]. Different from [1], we consider both a uniform linear array (ULA) and uniform planar array (UPA) of antennas at the BS. We adopt the classical narrowband ray-based channel model[2] [20], [21] as shown in Fig. 1. The downlink channel vector $\mathbf{h}_u \in \mathbb{C}^{M\times 1}$ for the u-th user can be described as

$$\mathbf{h}_u = \sum_{i=1}^{P_u} g_{u,i}\mathbf{a}\left(\phi_{u,i}, \theta_{u,i}\right), \tag{1}$$

where P_u is the number of dominant paths from the BS to the u-th user, $g_{u,i}$ is the complex gain of the i-th path of the u-th user, which is identically and independently distributed (IID) with zero mean and unit variance, and $\phi_{u,i}$ and $\theta_{u,i}$ are the azimuth and elevation AoDs of the i-th path of the u-th user, respectively. The steering vector $\mathbf{a}\left(\phi_{u,i}, \theta_{u,i}\right) \in \mathbb{C}^{M\times 1}$ denotes the antenna array response of the i-th path of the u-th user. For a ULA of antennas, the elevation AoD $\theta_{u,i}$ is neglected and the array response can be expressed as

$$\mathbf{a}\left(\phi_{u,i}\right) = \frac{1}{\sqrt{M}}\left[1, e^{j2\pi\frac{d}{\lambda}\sin\phi_{u,i}}, \cdots, e^{j2\pi\frac{d}{\lambda}(M-1)\sin\phi_{u,i}}\right]^{\mathrm{T}}, \tag{2}$$

where d is the antenna spacing at the BS, λ is the wavelength of the carrier frequency. For a UPA of antennas with M_1 horizontal antennas and M_2 vertical antennas ($M = M_1 \times M_2$), the array response can be expressed as

$$\begin{aligned}\mathbf{a}\left(\phi_{u,i}, \theta_{u,i}\right) = &\left[1, e^{j2\pi\frac{d}{\lambda}\sin\theta_{u,i}}, \cdots, e^{j2\pi\frac{d}{\lambda}(M_2-1)\sin\theta_{u,i}}\right]^{\mathrm{T}} \\ &\otimes\frac{1}{\sqrt{M}}\left[1, e^{j2\pi\frac{d}{\lambda}\cos\theta_{u,i}\sin\phi_{u,i}}, \cdots,\right. \\ &\left.\times\, e^{j2\pi\frac{d}{\lambda}(M_1-1)\cos\theta_{u,i}\sin\phi_{u,i}}\right]^{\mathrm{T}}. \end{aligned}\tag{3}$$

In matrix form with $\mathbf{A}_u = [\mathbf{a}\left(\phi_{u,1}, \theta_{u,1}\right), \mathbf{a}\left(\phi_{u,2}, \theta_{u,2}\right), \cdots, \mathbf{a}\left(\phi_{u,P_u}, \theta_{u,P_u}\right)] \in \mathbb{C}^{M\times P_u}$ and $\mathbf{g}_u = [g_{u,1}, g_{u,2}, \cdots, g_{u,P_u}]^{\mathrm{T}} \in \mathbb{C}^{P_u\times 1}$, we rewrite (1) as

$$\mathbf{h}_u = \mathbf{A}_u\mathbf{g}_u. \tag{4}$$

[2]The proposed technique can be extended to other channel models as long as they can characterize the multi-path propogation of physical channels such as [18] and [19].

Further, we express the MU-MIMO channel matrix as $\mathbf{H} = [\mathbf{h}_1, \mathbf{h}_2, \cdots, \mathbf{h}_U] \in \mathbb{C}^{M\times U}$.

B. Quantized Channel Feedback

In FDD systems, the downlink channel vector $\mathbf{h}_u$ is firstly estimated at the user side through downlink channel training. Although the pilot overhead for the downlink channel training is increased in massive MIMO systems, there are effective downlink training methods to solve this problem [21]–[23] by utilizing the angle-domain channel sparsity and the channel statistics. Thus, in this paper, each user is assumed to know its own channel vector. Then, the channel vector $\mathbf{h}_u$ is required to be fed back to the BS to perform downlink precoding. The channel vector $\mathbf{h}_u$ is firstly quantized and then fed back to the BS. The quantization of $\mathbf{h}_u \in \mathbb{C}^{M\times 1}$ is performed based on a quantization codebook $\mathcal{C}_u = \left\{\mathbf{c}_{u,1}, \mathbf{c}_{u,2}, \cdots, \mathbf{c}_{u,2^B}\right\}$, which consists of 2^B different M-dimension unit-norm column vectors, where B is the number of feedback bits. Details of codebook design will be discussed in Section III. The codebook $\mathcal{C}_u$ is known to both the BS and the u-th user. The channel vector $\mathbf{h}_u$ is quantized as a codeword $\mathbf{c}_{u,i_u}$, where the quantization index i_u is computed according to

$$i_u = \underset{i\in\{1,2,\cdots,2^B\}}{\arg\min}\ \sin^2\left(\measuredangle\left(\mathbf{h}_u, \mathbf{c}_{u,i}\right)\right) = \underset{i\in\{1,2,\cdots,2^B\}}{\arg\max}\left|\tilde{\mathbf{h}}_u^{\mathrm{H}}\mathbf{c}_{u,i}\right|^2, \tag{5}$$

where $\tilde{\mathbf{h}}_u = \frac{\mathbf{h}_u}{\|\mathbf{h}_u\|}$ is the channel direction.

Note that only the channel direction $\tilde{\mathbf{h}}_u$ is quantized, while the channel magnitude $\|\mathbf{h}_u\|$ is not quantized by the codebook $\mathcal{C}_u$. Channel magnitude information can be used to allocate power and rate across multiple channels, but it is just a scalar value and thus is also easy to be fed back (e.g., it can be uniformly quantized and then fed back). We follow the common assumption that the channel magnitude can be fed back to the BS perfectly so that we focus on the quantization of channel direction, which is more challenging for massive MIMO channel feedback. The quantization index i_u can be fed back from the u-th user to the BS through B dedicated bits. After receiving these B bits (thus the index i_u), the BS can obtain the quantized channel vector as $\hat{\mathbf{h}}_u = \|\mathbf{h}_u\|\,\mathbf{c}_{u,i_u}$. The MU-MIMO channel matrix obtained from the quantized channel feedback can be denoted as $\hat{\mathbf{H}} = \left[\hat{\mathbf{h}}_1, \hat{\mathbf{h}}_2, \cdots, \hat{\mathbf{h}}_U\right] \in \mathbb{C}^{M\times U}$.

C. Per-User Rate

The BS will perform the downlink precoding to eliminate inter-user interference based on the feedback MU-MIMO channel matrix $\hat{\mathbf{H}}$. We consider the commonly used ZF precoding. The transmit signal $\mathbf{x} \in \mathbb{C}^{M\times 1}$ after the ZF precoding is given by

$$\mathbf{x} = \sqrt{\frac{\gamma}{U}}\hat{\mathbf{V}}\mathbf{s}, \tag{6}$$

where γ is the transmit power, $\mathbf{s} = [s_1, s_2, \cdots, s_U]^{\mathrm{T}} \in \mathbb{C}^{U\times 1}$ is the signals intended for U users with the normalized power $\mathrm{E}\left[|s_i|^2\right] = 1$, and $\hat{\mathbf{V}} = [\hat{\mathbf{v}}_1, \hat{\mathbf{v}}_2, \cdots, \hat{\mathbf{v}}_U] \in \mathbb{C}^{M\times U}$ is the ZF precoding matrix consisting of U different M-dimension

unit-norm precoding vectors $\hat{\mathbf{v}}_i \in \mathbb{C}^{M\times 1}$, which is obtained as the normalized i-th column of $\hat{\mathbf{H}}^{\dagger}$, i.e., $\hat{\mathbf{v}}_i = \frac{\hat{\mathbf{H}}^{\dagger}(:,i)}{\left\|\hat{\mathbf{H}}^{\dagger}(:,i)\right\|}$.

The received signal at the u-th user can be described as

$$\begin{aligned} y_u &= \mathbf{h}_u^{\mathrm{H}}\mathbf{x} + n_u \\ &= \sqrt{\frac{\gamma}{U}}\mathbf{h}_u^{\mathrm{H}}\hat{\mathbf{v}}_u s_u + \sqrt{\frac{\gamma}{U}}\sum_{i=1,i\neq u}^{U}\mathbf{h}_u^{\mathrm{H}}\hat{\mathbf{v}}_i s_i + n_u, \end{aligned} \tag{7}$$

where n_u is the complex Gaussian noise at the u-th user with zero mean and unit variance. Thus, the signal-to-interference-plus-noise ratio (SINR) at the u-th user is

$$\mathrm{SINR}_u = \frac{\frac{\gamma}{U}\left|\mathbf{h}_u^{\mathrm{H}}\hat{\mathbf{v}}_u\right|^2}{1+\frac{\gamma}{U}\sum_{i=1,i\neq u}^{U}\left|\mathbf{h}_u^{\mathrm{H}}\hat{\mathbf{v}}_i\right|^2}. \tag{8}$$

Assuming Gaussian signaling and knowledge of SINR, the per-user rate $R_{\mathrm{Quantized}}$ with the quantized channel feedback technique is

$$\begin{aligned} R_{\mathrm{Quantized}} &= \mathrm{E}\left[\log_2(1+\mathrm{SINR}_u)\right] \\ &= \mathrm{E}\left[\log_2\left(1+\frac{\frac{\gamma}{U}\left|\mathbf{h}_u^{\mathrm{H}}\hat{\mathbf{v}}_u\right|^2}{1+\frac{\gamma}{U}\sum_{i=1,i\neq u}^{U}\left|\mathbf{h}_u^{\mathrm{H}}\hat{\mathbf{v}}_i\right|^2}\right)\right]. \end{aligned} \tag{9}$$

We can see that the per-user rate $R_{\mathrm{Quantized}}$ depends on the precoding matrix $\hat{\mathbf{V}}$, which is affected by the channel matrix $\hat{\mathbf{H}}$ obtained from the quantized channel feedback. In Section III, we propose an AoD-adaptive subspace codebook for the quantized channel feedback.

III. Proposed AoD-Adaptive Subspace Codebook

In this section, we firstly review the angle coherence time and then present the AoD-adaptive subspace codebook for channel feedback. We also provide a method to obtain the AoDs at the BS and the users during the angle coherence time.

A. Angle Coherence Time

Different from the traditional channel coherence time, the angle coherence time is defined as a comparably long time, during which the AoDs can be regarded as static. Specifically, the path AoD $(\phi_{u,i},\theta_{u,i})$ in (1) mainly depends on the surrounding obstacles around the BS, which may not physically change their positions often. On the contrary, the path gain $g_{u,i}$ characterizing the i-th dominant path of the u-th user depends on a number of unresolvable paths, each of which is generated by a scatter surrounding the user. Therefore, path gains vary much faster than the path AoDs [6]. Accordingly, the angle coherence time is much longer than the traditional channel coherence time.

B. Proposed AoD-Adaptive Subspace Codebook

During the comparably long angle coherence time, the channel vector $\mathbf{h}_u$ is distributed in the *channel subspace*. Specifically, as shown in (1) and (4), the channel vector $\mathbf{h}_u$ between the BS and the u-th user is composed of P_u paths as $\mathbf{h}_u = \sum_{i=1}^{P_u} g_{u,i}\mathbf{a}\left(\phi_{u,i},\theta_{u,i}\right) = \mathbf{A}_u\mathbf{g}_u$. Therefore, the channel vector $\mathbf{h}_u$ is actually distributed in the column space of $\mathbf{A}_u \in \mathbb{C}^{M\times P_u}$, which is spanned by $\mathbf{A}_u$'s P_u column vectors.

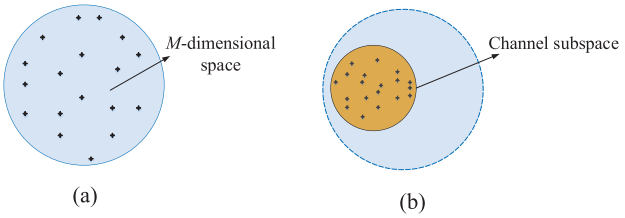

Fig. 2. Codebook comparison: (a) the traditional RVQ codebook; (b) the proposed AoD-adaptive subspace codebook. Each dot in the figure denotes a codeword in the codebook, which is randomly distributed in the M-dimension space and the channel subspace in (a) and (b), respectively.

Due to the limited scattering of millimeter-wave signals, the number of dominant paths P_u is much smaller (e.g., $P_u = 2 \sim 8$ for 6-60GHz [24]) than the number of BS antennas M (e.g., $M = 128, 256$). We also expect this to be true even with massive MIMO in sub-6GHz, since the number of dominant paths P_u depends on the clusters of scatters around the BS whose number is usually limited[3]. Therefore, the column space of $\mathbf{A}_u$, which is completely determined by $P_u(\ll M)$ path AoDs $\{(\phi_{u,i},\theta_{u,i})\}_{i=1}^{P_u}$, is only a subspace of the full M-dimension space. This subspace is referred to as the channel subspace.

Based on the channel subspace in the angle coherence time, we can design an AoD-adaptive subspace codebook to quantize the channel vector in a better way, where quantization vectors (i.e., codewords) are exactly distributed in the channel subspace as shown in Fig. 2. Specifically, we assume that the quantized AoDs $\left\{(\hat{\phi}_{u,i},\hat{\theta}_{u,i})\right\}_{i=1}^{P_u}$ can be obtained at both the BS and the u-th user (how to obtain the AoDs will be discussed later in the next subsection). After the BS and the u-th user obtaining the quantized AoDs, they can generate the steering matrix as $\hat{\mathbf{A}}_u = \left[\mathbf{a}\left(\hat{\phi}_{u,1},\hat{\theta}_{u,1}\right),\mathbf{a}\left(\hat{\phi}_{u,2},\hat{\theta}_{u,2}\right),\cdots,\mathbf{a}\left(\hat{\phi}_{u,P_u},\hat{\theta}_{u,P_u}\right)\right] \in \mathbb{C}^{M\times P_u}$. Then, the quantization vector $\mathbf{c}_{u,i}$ of the proposed AoD-adaptive subspace codebook can be designed as

$$\mathbf{c}_{u,i} = \hat{\mathbf{A}}_u\mathbf{w}_{u,i}, \tag{10}$$

where the unit-norm vector $\mathbf{w}_{u,i} \in \mathbb{C}^{P_u\times 1}$ is chosen from a vector quantization codebook $\mathcal{W}_u = \left\{\mathbf{w}_{u,1},\mathbf{w}_{u,2},\cdots,\mathbf{w}_{u,2^B}\right\}$. $\mathcal{W}_u$ is assumed to be a random vector quantization (RVQ) codebook, which is randomly generated by selecting vectors independently from the uniform distribution on the complex unit sphere [5], [25]. Similar to [1], we consider the RVQ framework to enable the performance analysis of the proposed AoD-adaptive subspace codebook. In practice, $\mathbf{w}_{u,i}$ can be chosen from other practical codebooks, such as the Lloyd algorithm based vector quantization codebook [26], [27]. The Lloyd algorithm has already been used as a standard tool for the feedback codebook design [15]. The Lloyd algorithm can

[3]Note that P_u only depends on the scattering geometry around the BS. Since the BS is usually located at high towers or mounts, the number of significant scatters around the BS is limited. Besides, in the widely used 3GPP spatial channel model (SCM) for sub-6 GHz [18], the number of dominant channel paths for both macro cell and micro cell is set as 10-20. Therefore, it is reasonable to assume than $P_u \ll M$ in massive MIMO systems.

be applied to the proposed AoD-adaptive subspace codebook by designing a vector quantization codebook $\mathcal{W}_u$ to minimize the average distortion

$$d_{\text{Lloyd}}(\mathcal{W}_u) = \mathrm{E}\left[\|\tilde{\mathbf{g}}_u\|^2 - \max_{\mathbf{w}_{u,i}\in\mathcal{W}_u} \tilde{\mathbf{g}}_u^{\mathrm{H}}\mathbf{w}_{u,i}\right], \quad (11)$$

where $\tilde{\mathbf{g}}_u = \mathbf{g}_u/\|\mathbf{g}_u\|$ is the normalized path gain vector. The Lloyd algorithm can be easily implemented by generating several test channel path gain vectors $\mathbf{g}_u$ and iteratively refining the vector quantization codebook $\mathcal{W}_u$ [15]. The performance of the proposed AoD-adaptive subspace codebook under the RVQ framework is very close to that under the Lloyd framework, which will be shown through simulations.

Note that the quantization vector $\mathbf{c}_{u,i}$ is a unit-norm vector, i.e., $\|\mathbf{c}_{u,i}\| = \left\|\hat{\mathbf{A}}_u\mathbf{w}_{u,i}\right\| = 1$ which can be proved as

$$\begin{aligned}\left\|\hat{\mathbf{A}}_u\mathbf{w}_{u,i}\right\|^2 &= \left\|\Sigma_{p=1}^{P_u}\mathbf{a}\left(\hat{\phi}_{u,p},\hat{\theta}_{u,p}\right)w_{u,i,p}\right\|^2 \\ &\overset{M\to\infty}{=} \Sigma_{p=1}^{P_u}\left\|\mathbf{a}\left(\hat{\phi}_{u,p},\hat{\theta}_{u,p}\right)w_{u,i,p}\right\|^2 \\ &= \Sigma_{p=1}^{P_u}|w_{u,i,p}|^2 = \|\mathbf{w}_{u,i}\|^2 = 1, \quad (12)\end{aligned}$$

where the second equation is true due to the orthogonality among column vectors $\mathbf{a}\left(\hat{\phi}_{u,p},\hat{\theta}_{u,p}\right)$ of $\hat{\mathbf{A}}_u$ when $M\to\infty$, which is proved in Lemma 3 shown in Appendix I.

We evaluate the computational complexity of the proposed quantized feedback technique using the AoD-adaptive subspace codebook, which consists of two parts. The first part is the computations of quantization index i_u in (5). Since the size of AoD-adaptive subspace codebook is proportional to 2^P as will be shown in Section V, the complexity for computing the quantization index is $\mathcal{O}(M2^P)$. The other part of computational complexity is required by the update of the proposed codebook according to the AoD information in each angle coherence time. According to the codewords design in (10), the computational complexity for every update of the proposed codebook is $\mathcal{O}(MP2^P)$. Note that the angle coherence time is much longer than the channel coherence time. For example, when the angle coherence time is 10 times of the channel coherence time [6], the average complexity for the codebook update is $\mathcal{O}(MP2^P/10)$. By adding these two parts of complexity together, we can obtain that the overall complexity of the proposed quantized feedback technique using the AoD-adaptive subspace codebook is $\mathcal{O}(M2^P + MP2^P/10)$. For the traditional channel feedback scheme, the size of feedback codebook should be proportional to 2^M [4], [5]. Therefore, the traditional channel feedback scheme has the complexity $\mathcal{O}(M2^M)$. Since $P \ll M$, the complexity of the proposed quantized feedback technique using the AoD-adaptive subspace codebook is smaller than that of the traditional channel feedback scheme.

C. AoD Acquisition

In this subsection, we will describe how the BS and users obtain AoDs within the angle coherence time. As presented in Subsection II-B, users are assumed to have obtained their channel estimates. Then, the users can estimate the AoDs from the channel estimates by using the multiple signal classification (MUSIC) algorithm [28]. Specifically, the correlation matrix of channel vector $\mathbf{h}_u$ of the u-th user can be calculated as $\mathbf{R}_u = \mathrm{E}[\mathbf{h}_u\mathbf{h}_u^{\mathrm{H}}]$, where the expectation is estimated using the sample average obtained over several channel estimates during the angle coherence time. Based on $\mathbf{R}_u$, AoDs can be estimated by using the classical MUSIC algorithm [28]. Since the BS also needs to know AoDs to generate the proposed AoD-adaptive subspace codebook $\mathcal{C}_u$, the estimated AoDs have to be fed back to the BS. A common uniform quantization can be adopted to quantize each AoD with B_0 bits. Since the angle coherence time is much longer than the channel coherence time, the average overhead for AoD feedback is not high.

IV. Performance Analysis of The Proposed AoD-Adaptive Subspace Codebook

In this section, we evaluate the performance of the proposed AoD-adaptive subspace codebook in the large-dimension regime, i.e., the number of the BS antennas M is sufficiently large. We firstly calculate the rate gap between the ideal case of the perfect CSIT and the practical case of the proposed quantized feedback technique using the AoD-adaptive subspace codebook. Then, we analyze the quantization error of the proposed codebook which dominates the rate gap. Finally, we derive a lower bound of the required number of feedback bits to limit the rate gap within a constant value.

A. Rate Gap of Quantized Channel Feedback

In the ideal case of the perfect CSIT at the BS, i.e., $\hat{\mathbf{H}} = \mathbf{H}$, the ZF precoding vector $\mathbf{v}_{\text{Ideal},i} \in \mathbb{C}^{M\times 1}$ is obtained as the normalized i-th column of $\mathbf{H}^{\dagger}$. Thus, $\mathbf{v}_{\text{Ideal},i}$ is orthogonal to the u-th user's channel vector $\mathbf{h}_u$ for any $i \neq u$, i.e., the inter-user interference $|\mathbf{h}_u^{\mathrm{H}}\mathbf{v}_{\text{Ideal},i}| = 0$. The corresponding per-user rate is

$$R_{\text{Ideal}} = \mathrm{E}\left[\log_2\left(1+\frac{\gamma}{U}|\mathbf{h}_u^{\mathrm{H}}\mathbf{v}_{\text{Ideal},u}|^2\right)\right]. \quad (13)$$

In the practical case of the quantized channel feedback technique, the BS can only obtain the quantized channel $\hat{\mathbf{H}}$, which is not identical to the ideal channel $\mathbf{H}$. The ZF precoding is performed based on $\hat{\mathbf{H}}$, and the precoding vector $\hat{\mathbf{v}}_i \in \mathbb{C}^{M\times 1}$ is obtained as the normalized i-th column of $\hat{\mathbf{H}}^{\dagger}$. Since the inter-user interference is nonzero now (i.e., $|\mathbf{h}_u^{\mathrm{H}}\hat{\mathbf{v}}_i| \neq 0$), the degraded per-user rate $R_{\text{Quantized}}$ is shown in (9). Following [5, Th. 1], the rate gap $\Delta R_{\text{Quantized}} = R_{\text{Ideal}} - R_{\text{Quantized}}$ can be upper bounded as

$$\Delta R_{\text{Quantized}} \leq \log_2\left(1+(U-1)\frac{\gamma}{U}\mathrm{E}\left[\|\mathbf{h}_u\|^2\right]\mathrm{E}\left[\left|\tilde{\mathbf{h}}_u^{\mathrm{H}}\hat{\mathbf{v}}_i\right|^2\right]\right), \quad (14)$$

where $\tilde{\mathbf{h}}_u$ is the normalized channel vector in (5), and the inter-user interference $\mathrm{E}\left[\left|\tilde{\mathbf{h}}_u^{\mathrm{H}}\hat{\mathbf{v}}_i\right|^2\right]$ in (14) is expressed in the following Lemma 1.

Lemma 1: The inter-user interference $\mathrm{E}\left[\left|\tilde{\mathbf{h}}_u^{\mathrm{H}}\hat{\mathbf{v}}_i\right|^2\right]$ is dominated by the quantization error $\mathrm{E}\left[\sin^2\left(\measuredangle\left(\tilde{\mathbf{h}}_u,\hat{\mathbf{h}}_u\right)\right)\right]$,

i.e., for any $u \neq i$,

$$\mathrm{E}\left[\left|\tilde{\mathbf{h}}_u^{\mathrm{H}}\hat{\mathbf{v}}_i\right|^2\right] = \alpha \mathrm{E}\left[\sin^2\left(\measuredangle\left(\tilde{\mathbf{h}}_u, \hat{\mathbf{h}}_u\right)\right)\right], \tag{15}$$

where α is a scale factor.

Proof: $\tilde{\mathbf{h}}_u = \frac{\mathbf{h}_u}{\|\mathbf{h}_u\|}$ is the normalized channel vector of the u-th user. $\hat{\mathbf{h}}_u = \|\mathbf{h}_u\| \mathbf{c}_{u,i_u}$ is the quantized channel vector, where $\mathbf{c}_{u,i_u}$ is the unit-norm quantization vector with index i_u in the codebook $\mathcal{C}_u$. We define $Z = \sin^2\left(\measuredangle\left(\tilde{\mathbf{h}}_u, \hat{\mathbf{h}}_u\right)\right) = \sin^2\left(\measuredangle\left(\tilde{\mathbf{h}}_u, \mathbf{c}_{u,i_u}\right)\right)$. Since the size of the codebook is limited, it is clear that $Z \neq 0$. Thus, the normalized channel vector $\tilde{\mathbf{h}}_u$ can be decomposed along two orthogonal directions, one is the direction of quantization vector $\mathbf{c}_{u,i_u}$, and the other is in the nullspace of $\mathbf{c}_{u,i_u}$ [5]:

$$\tilde{\mathbf{h}}_u = \sqrt{1-Z}\mathbf{c}_{u,i_u} + \sqrt{Z}\mathbf{q}, \tag{16}$$

where $\mathbf{q}$ is an unit-norm vector distributed in the null space of $\mathbf{c}_{u,i_u}$. Utilizing the orthogonality between $\mathbf{c}_{u,i_u}$ and $\mathbf{q}$, we have

$$\left|\tilde{\mathbf{h}}_u^{\mathrm{H}}\hat{\mathbf{v}}_i\right|^2 = (1-Z)\left|\mathbf{c}_{u,i_u}^{\mathrm{H}}\hat{\mathbf{v}}_i\right|^2 + Z\left|\mathbf{q}^{\mathrm{H}}\hat{\mathbf{v}}_i\right|^2. \tag{17}$$

Since $\hat{\mathbf{v}}_i$ is the ZF precoding vector, which is orthogonal to $\hat{\mathbf{h}}_u = \|\mathbf{h}_u\| \mathbf{c}_{u,i_u}$, we have

$$\left|\tilde{\mathbf{h}}_u^{\mathrm{H}}\hat{\mathbf{v}}_i\right|^2 = Z\left|\mathbf{q}^{\mathrm{H}}\hat{\mathbf{v}}_i\right|^2. \tag{18}$$

According to the results of [5], Z is independent with $\mathbf{q}$ and $\hat{\mathbf{v}}_i$, so we have

$$\mathrm{E}\left[\left|\tilde{\mathbf{h}}_u^{\mathrm{H}}\hat{\mathbf{v}}_i\right|^2\right] = \mathrm{E}[Z]\,\mathrm{E}\left[\left|\mathbf{q}^{\mathrm{H}}\hat{\mathbf{v}}_i\right|^2\right]. \tag{19}$$

By denoting $\alpha = \mathrm{E}\left[\left|\mathbf{q}^{\mathrm{H}}\hat{\mathbf{v}}_i\right|^2\right]$, we can obtain (15). ■

Lemma 2: The scale factor can be upper bounded as $\alpha \leq \frac{1}{P-1}$ when $\hat{\mathbf{A}}_u = \mathbf{A}_u$ and $M \to \infty$, where P is the number of dominant paths per user.

Proof: The scale factor α denoting the scaling of the inter-user interference $\mathrm{E}\left[\left|\tilde{\mathbf{h}}_u^{\mathrm{H}}\hat{\mathbf{v}}_i\right|^2\right]$ in (15) can achieve its upper bound in an extreme case, where the channels of all the U users are strongly correlated. In this case, U users share the same clusters around the BS in the ray-based channel model, i.e., $P_1 = P_2 = \cdots = P_U = P$ and $\mathbf{A}_1 = \mathbf{A}_2 = \cdots = \mathbf{A}_U = \mathbf{A}$. Thus, we can omit the subscript u of P_u, $\mathbf{A}_u$ and $\hat{\mathbf{A}}_u$ in this proof.

Firstly, we look at the two vectors $\mathbf{q}$ and $\hat{\mathbf{v}}_i$, respectively. When $\hat{\mathbf{A}}_u = \mathbf{A}_u$, i.e., $\hat{\mathbf{A}} = \mathbf{A}$, as we presented in Section III-B, both the feedback channel vector $\hat{\mathbf{h}}_u$ and normalized channel vector $\tilde{\mathbf{h}}_u$ are distributed in the column-space of $\mathbf{A}$, i.e., the channel subspace. Since $\tilde{\mathbf{h}}_u$ can be orthogonally discomposed along the directions of $\hat{\mathbf{h}}_u$ and $\mathbf{q}$, $\mathbf{q}$ should also be distributed in the column-space of $\mathbf{A}$. Thus, $\mathbf{q}$ can be expressed as $\mathbf{q} = \frac{\mathbf{At}}{\|\mathbf{At}\|}$, where $\mathbf{t} \in \mathbb{C}^{P\times 1}$ and we can assume that $\|\mathbf{t}\| = 1$ without loss of generality. Similar to the proof in (12), utilizing the orthogonality among column vectors of $\mathbf{A}$ when $M \to \infty$, we have $\|\mathbf{At}\| \overset{M\to\infty}{=} \|\mathbf{t}\| = 1$. Therefore, $\mathbf{q}$ can be expressed as $\mathbf{q} \overset{M\to\infty}{=} \mathbf{At}$. The precoding vector $\hat{\mathbf{v}}_i$ is the normalized i-th column of $\mathbf{H}^{\dagger} = \mathbf{H}(\mathbf{H}^{\mathrm{H}}\mathbf{H})^{-1}$. By using $\mathbf{H} = [\mathbf{h}_1, \mathbf{h}_2, \cdots, \mathbf{h}_U] = \mathbf{A}[\mathbf{g}_1, \mathbf{g}_2, \cdots, \mathbf{g}_P] = \mathbf{AG}$, we can express the precoding vector as $\hat{\mathbf{v}}_i = \frac{\mathbf{Au}}{\|\mathbf{Au}\|}$ where $\mathbf{u}$ is assumed as a unit-norm vector without loss of generality. Similar to the proof in (12), utilizing the orthogonality among column vectors of $\mathbf{A}$ when $M \to \infty$, we have $\|\mathbf{Au}\| \overset{M\to\infty}{=} \|\mathbf{u}\| = 1$. Therefore, $\hat{\mathbf{v}}_i$ can be expressed as $\hat{\mathbf{v}}_i \overset{M\to\infty}{=} \mathbf{Au}$.

Then, we can calculate

$$\mathrm{E}\left[\left|\mathbf{q}^{\mathrm{H}}\hat{\mathbf{v}}_i\right|^2\right] \overset{M\to\infty}{=} \mathrm{E}\left[\left|\mathbf{t}^{\mathrm{H}}\mathbf{A}^{\mathrm{H}}\mathbf{Au}\right|^2\right] \overset{M\to\infty}{=} \mathrm{E}\left[\left|\mathbf{t}^{\mathrm{H}}\mathbf{u}\right|^2\right]. \tag{20}$$

where the second equation follows from the result $\mathbf{A}^{\mathrm{H}}\mathbf{A} \overset{M\to\infty}{=} \mathbf{I}_P$ in Lemma 3 in Appendix I. By substituting the following result presented in Lemma 4 in Appendix II that

$$\mathrm{E}\left[\left|\mathbf{t}^{\mathrm{H}}\mathbf{u}\right|^2\right] = \frac{1}{P-1}, \tag{21}$$

we obtain the upper bound on the scale factor as

$$\alpha \leq \mathrm{E}\left[\left|\mathbf{q}^{\mathrm{H}}\hat{\mathbf{v}}_i\right|^2\right] \overset{M\to\infty}{=} \frac{1}{P-1}. \tag{22}$$

■

B. Quantization Error

In this subsection, we compute the quantization error $\mathrm{E}\left[\sin^2\left(\measuredangle\left(\tilde{\mathbf{h}}_u, \hat{\mathbf{h}}_u\right)\right)\right]$ in (15) in the large-dimension regime when the proposed AoD-adaptive subspace codebook is considered. For the rest of this section, we omit the subscript u for simplicity. Since $\left\|\tilde{\mathbf{h}}\right\| = 1$ and $\frac{\hat{\mathbf{h}}}{\|\hat{\mathbf{h}}\|} = \mathbf{c}_i$, the quantization error $\mathrm{E}\left[\sin^2\left(\measuredangle\left(\tilde{\mathbf{h}}, \hat{\mathbf{h}}\right)\right)\right]$ can be expressed as

$$\mathrm{E}\left[\sin^2\left(\measuredangle\left(\tilde{\mathbf{h}}, \hat{\mathbf{h}}\right)\right)\right] = 1 - \mathrm{E}\left[\left|\tilde{\mathbf{h}}^{\mathrm{H}}\mathbf{c}_i\right|^2\right], \tag{23}$$

where $\tilde{\mathbf{h}} = \frac{\mathbf{Ag}}{\|\mathbf{h}\|}$ according to (4). Similar to the proof in (12), it is easy to show that $\|\mathbf{h}\| = \|\mathbf{Ag}\| \overset{M\to\infty}{=} \|\mathbf{g}\|$. By denoting $\tilde{\mathbf{g}} = \frac{\mathbf{g}}{\|\mathbf{g}\|}$, we have $\tilde{\mathbf{h}} \overset{M\to\infty}{=} \frac{\mathbf{Ag}}{\|\mathbf{g}\|} \overset{M\to\infty}{=} \mathbf{A}\tilde{\mathbf{g}}$. Combining $\tilde{\mathbf{h}} \overset{M\to\infty}{=} \mathbf{A}\tilde{\mathbf{g}}$ and (10), we have

$$\begin{aligned}\mathrm{E}\left[\left|\tilde{\mathbf{h}}^{\mathrm{H}}\mathbf{c}_i\right|^2\right] &\overset{M\to\infty}{=} \mathrm{E}\left[\left|\tilde{\mathbf{g}}^{\mathrm{H}}\mathbf{A}^{\mathrm{H}}\hat{\mathbf{A}}\mathbf{w}_i\right|^2\right] \\ &\overset{M\to\infty}{=} \mathrm{E}\left[\left|\mathcal{K}\tilde{\mathbf{g}}^{\mathrm{H}}\mathbf{w}_i\right|^2\right] \overset{M\to\infty}{=} |\mathcal{K}|^2\,\mathrm{E}\left[\left|\tilde{\mathbf{g}}^{\mathrm{H}}\mathbf{w}_i\right|^2\right],\end{aligned} \tag{24}$$

where the second equation is true due to $\mathbf{A}^{\mathrm{H}}\hat{\mathbf{A}} \overset{M\to\infty}{=} \mathcal{K}\mathbf{I}_P$ as proved in Lemma 3 (see Appendix I). Since both $\tilde{\mathbf{g}}$ and $\mathbf{w}_i$ are isotropically distributed vectors on the P-dimension unit sphere, we have [5]

$$\mathrm{E}\left[\left|\tilde{\mathbf{g}}^{\mathrm{H}}\mathbf{w}_i\right|^2\right] > 1 - 2^{-\frac{B}{P-1}}. \tag{25}$$

Combining (23), (24), and (25), we have

$$\mathrm{E}\left[\sin^2\left(\measuredangle\left(\tilde{\mathbf{h}}, \hat{\mathbf{h}}\right)\right)\right] < 1 - |\mathcal{K}|^2\left(1 - 2^{-\frac{B}{P-1}}\right). \tag{26}$$

By substituting $|\mathcal{K}|^2 \geq 1 - \frac{M^2}{3}\left(\pi\frac{d}{\lambda}\right)^2 r^2 2^{-2B_0}$ (44) in Appendix I into (26) and denoting $\beta = \frac{M^2}{3}(\pi\frac{d}{\lambda})^2 r^2 2^{-2B_0}$,

we can obtain the upper bound on the quantization error $\mathrm{E}\left[\sin^2\left(\measuredangle\left(\tilde{\mathbf{h}},\hat{\mathbf{h}}\right)\right)\right]$ as

$$\mathrm{E}\left[\sin^2\left(\measuredangle\left(\tilde{\mathbf{h}},\hat{\mathbf{h}}\right)\right)\right] < \beta(1-2^{-\frac{B}{P-1}})+2^{-\frac{B}{P-1}}. \quad (27)$$

We can observe from (27) that a small β leads to a small quantization error due to $2^{-\frac{B}{P-1}} \ll 1$. That means a small β, i.e., a large number of AoD quantization bits B_0 can achieve a small quantization error. In addition, (27) can be rewritten as

$$\mathrm{E}\left[\sin^2\left(\measuredangle\left(\tilde{\mathbf{h}},\hat{\mathbf{h}}\right)\right)\right] < (1-\beta)2^{-\frac{B}{P-1}}+\beta, \quad (28)$$

where a small quantization error can be achieved with a large number of channel feedback bits B since $\beta \ll 1$ with a reasonably designed B_0.

C. Feedback Bits

Finally, based on the previous analytical results, we will evaluate the required number of feedback bits B to guarantee a constant rate gap $\Delta R_{\text{Quantized}} \leq \log_2 b$ bps/Hz. By combining (14), (15), and (28), we can obtain the rate gap as

$$\Delta R_{\text{Quantized}} \leq \log_2\left(1+\frac{(U-1)\gamma}{U}\mathrm{E}\left[\|\mathbf{h}\|^2\right]\alpha(1-\beta)2^{-\frac{B}{P-1}} + \frac{(U-1)\gamma}{U}\mathrm{E}\left[\|\mathbf{h}\|^2\right]\alpha\beta\right). \quad (29)$$

Let $\Delta R_{\text{Quantized}} \leq \log_2\left(1+\frac{(U-1)\gamma}{U}\mathrm{E}\left[\|\mathbf{h}\|^2\right]\alpha(1-\beta)2^{-\frac{B}{P-1}} + \frac{(U-1)\gamma}{U}\mathrm{E}\left[\|\mathbf{h}\|^2\right]\alpha\beta\right) \leq \log_2 b$ bps/Hz, then the number of feedback bits B should scale according to

$$B \geq \frac{P-1}{3}\text{SNR}+(P-1)\log_2\frac{(U-1)\alpha(1-\beta)}{b-1-\xi}, \quad (30)$$

where $\text{SNR} = 10\log_{10}\frac{\gamma}{U}\mathrm{E}\left[\|\mathbf{h}\|^2\right]$ is the signal-to-noise-ratio (SNR) at the receiver and $\xi = \frac{(U-1)\gamma}{U}\mathrm{E}\left[\|\mathbf{h}\|^2\right]\alpha\beta$. Note that ξ is also related to the receiver SNR.

Remark 1: We observe from (30) that the relationship between B and SNR is very complicated due to ξ. However, since ξ depends on β, which is usually very small, B in (30) is dominated by the first item $\frac{P-1}{3}$SNR when SNR increases. That is to say, the required number of feedback bits B approximately scales linearly with the number of dominant paths P when SNR increases. If we assume that the perfect AoD information is known, i.e., $\beta = 0$, we have $\xi = 0$ and the required number of feedback bits $B \geq \frac{P-1}{3}\text{SNR} + (P-1)\log_2\frac{(U-1)\alpha}{b-1}$ as shown in [1]. With the perfect AoD information, B scales exactly linearly with P. Since $P \ll M$, the proposed AoD-adaptive subspace codebook can significantly reduce the feedback overhead.

V. Quantized Channel Feedback vs. Analog Channel Feedback

In this section, we firstly propose a novel analog channel feedback technique based on the channel subspace. Then, we quantitatively analyze the proposed channel subspace based analog feedback technique by evaluating the rate gap between the ideal case of the perfect CSIT and the practical case of the proposed analog feedback technique. Finally, we compare the proposed quantized feedback technique using the AoD-adaptive subspace codebook with the channel subspace based analog feedback technique.

A. Analog Channel Feedback Technique

Analog linear modulation may be used for the channel feedback without quantization (i.e., analog channel feedback) due to its circumvention of codebook complexities and delays associated with quantization, source coding and channel coding in quantized channel feedback techniques [29]. In the traditional analog channel feedback technique, each element of the channel vector $\mathbf{h}_u$ in (1) is fed back without quantization through the uplink noisy channel [29], [30]. Previous work has compared the traditional analog feedback technique with the quantized feedback technique using the RVQ codebook [31]. It has been shown that the quantized feedback technique outperforms the analog feedback technique if the channel rate (of uplink) is larger than the source rate (i.e., downlink CSI) and the source is IID Gaussian over an AWGN channel. This is because the effect of feedback noise vanishes at high SNR for the quantized channel feedback technique but does not do so for the analog channel feedback technique.

Different from the traditional analog channel feedback technique [29], [30], in this paper, we propose a novel analog channel feedback technique based on the channel subspace. During the angle coherence time, we can assume that path AoDs, i.e., the steering matrix $\mathbf{A}_u$ of the u-th user is known to the BS and the u-th user. In this case, since $\mathbf{h}_u = \mathbf{A}_u\mathbf{g}_u$, only the elements of the $P_u \times 1$ path gain vector $\mathbf{g}_u$ are fed back through noisy uplink channel. The observation of the path gain vector $\mathbf{g}_u$ at the BS after noisy uplink channel is given by [31]

$$\mathbf{z}_u = \sqrt{\mu\gamma_{\text{U}}}\mathbf{g}_u + \mathbf{n}_{\text{U},u}, \quad (31)$$

where γ_{U} is the uplink SNR (not in dB) and $\mathbf{n}_{\text{U},u}$ is the uplink complex Gaussian noise, where each element has zero mean and unit variance. The scale factor μ denotes the number of channel uses to feedback one element of the path gain vector $\mathbf{g}_u$. The MMSE estimate of the path gain vector at the BS is $\check{\mathbf{g}}_u = \frac{\sqrt{\mu\gamma_{\text{U}}}}{1+\mu\gamma_{\text{U}}}\mathbf{z}_u$. We denote $\mathbf{g}_u = \check{\mathbf{g}}_u + \mathbf{e}_{g,u}$, where $\check{\mathbf{g}}_u$ and $\mathbf{e}_{g,u}$ are mutually independent and have Gaussian components with zero mean and variance $\mu\gamma_{\text{U}}\sigma^2_{e_{g,u}}$ and $\sigma^2_{e_{g,u}} = (1+\mu\gamma_{\text{U}})^{-1}$. Then, by utilizing the path AoD information, i.e., steering matrix $\mathbf{A}_u$, the BS can recover the channel vector $\check{\mathbf{h}}_u$ obtained from the proposed channel subspace based analog feedback as

$$\check{\mathbf{h}}_u = \mathbf{A}_u\check{\mathbf{g}}_u. \quad (32)$$

Therefore we can rewrite the channel vector $\mathbf{h}_u$ as

$$\mathbf{h}_u = \mathbf{A}_u\mathbf{g}_u = \check{\mathbf{h}}_u + \mathbf{A}_u\mathbf{e}_{g,u}. \quad (33)$$

The MU-MIMO channel matrix obtained from the analog channel feedback can be denoted as $\check{\mathbf{H}} = \left[\check{\mathbf{h}}_1, \check{\mathbf{h}}_2, \cdots, \check{\mathbf{h}}_U\right] \in \mathbb{C}^{M\times U}$.

B. Rate Gap of the Analog Channel Feedback

Similar to the quantized channel feedback technique, we consider the ZF precoding for downlink transmission, which is realized based on the MU-MIMO channel matrix $\check{\mathbf{H}}$ obtained from the proposed channel subspace based analog feedback technique. The ZF precoding matrix $\check{\mathbf{V}} = [\check{\mathbf{v}}_1, \check{\mathbf{v}}_2, \cdots, \check{\mathbf{v}}_U] \in \mathbb{C}^{M\times U}$ consists of U different M-dimension unit-norm precoding vectors $\check{\mathbf{v}}_i \in \mathbb{C}^{M\times 1}$, which is obtained by the normalization of the i-th column of $\check{\mathbf{H}}^{\dagger}$, i.e., $\check{\mathbf{v}}_i = \frac{\check{\mathbf{H}}^{\dagger}(:,i)}{\left\|\check{\mathbf{H}}^{\dagger}(:,i)\right\|}$. After the downlink channel, the received signal at the u-th user can be described as

$$\begin{aligned} y_u &= \sqrt{\frac{\gamma}{U}}\mathbf{h}_u^{\mathrm{H}}\check{\mathbf{v}}_u s_u + \sqrt{\frac{\gamma}{U}}\sum_{i=1,i\neq u}^{U}\mathbf{h}_u^{\mathrm{H}}\check{\mathbf{v}}_i s_i + n_u \\ &\overset{(a)}{=} \sqrt{\frac{\gamma}{U}}\mathbf{h}_u^{\mathrm{H}}\check{\mathbf{v}}_u s_u + \sqrt{\frac{\gamma}{U}}\sum_{i=1,i\neq u}^{U}\mathbf{e}_{g,u}^{\mathrm{H}}\mathbf{A}_u^{\mathrm{H}}\check{\mathbf{v}}_i s_i + n_u, \quad (34) \end{aligned}$$

where (a) is obtained by substituting (33) and $\check{\mathbf{h}}_u^{\mathrm{H}}\check{\mathbf{v}}_i = 0$ ($\forall i \neq u$). The per-user rate of the proposed channel subspace based analog feedback technique is

$$R_{\text{Analog}} = \mathrm{E}\left[\log_2\left(1+\frac{\frac{\gamma}{U}\left|\mathbf{h}_u^{\mathrm{H}}\check{\mathbf{v}}_u\right|^2}{1+\frac{\gamma}{U}\sum_{i=1,i\neq u}^{U}\left|\mathbf{e}_{g,u}^{\mathrm{H}}\mathbf{A}_u^{\mathrm{H}}\check{\mathbf{v}}_i\right|^2}\right)\right]. \quad (35)$$

Defining the rate gap between the ideal case of the perfect CSIT and the practical case of the analog channel feedback technique as $\Delta R_{\text{Analog}} = R_{\text{Ideal}} - R_{\text{Analog}}$, we have

$$\begin{aligned} \Delta R_{\text{Analog}} &= \mathrm{E}\left[\log_2\left(1+\frac{\gamma}{U}\left|\mathbf{h}_u^{\mathrm{H}}\mathbf{v}_{\text{Ideal},i}\right|^2\right)\right] \\ &\quad -\mathrm{E}\left[\log_2\left(1+\frac{\frac{\gamma}{U}\left|\mathbf{h}_u^{\mathrm{H}}\check{\mathbf{v}}_u\right|^2}{1+\frac{\gamma}{U}\sum_{i=1,i\neq u}^{U}\left|\mathbf{e}_{g,u}^{\mathrm{H}}\mathbf{A}_u^{\mathrm{H}}\check{\mathbf{v}}_i\right|^2}\right)\right]. \end{aligned} \quad (36)$$

Following [31], ΔR_{Analog} can be upper bounded as

$$\Delta R_{\text{Analog}} \leq \log_2\left(1+(U-1)\frac{\gamma}{U}\mathrm{E}\left[\left|\mathbf{e}_{g,u}^{\mathrm{H}}\mathbf{A}_u^{\mathrm{H}}\check{\mathbf{v}}_i\right|^2\right]\right). \quad (37)$$

Next we evaluate the upper bound on the inter-user interference $\mathrm{E}\left[\left|\mathbf{e}_{g,u}^{\mathrm{H}}\mathbf{A}_u^{\mathrm{H}}\check{\mathbf{v}}_i\right|^2\right]$. As is clear, the inter-user interference $\mathrm{E}\left[\left|\mathbf{e}_{g,u}^{\mathrm{H}}\mathbf{A}_u^{\mathrm{H}}\check{\mathbf{v}}_i\right|^2\right]$ can achieve its upper bound in an extreme case, where the channels of all the U users are strongly correlated, i.e., the U users share the same clusters around the BS. In this extreme case, $P_1 = P_2 = \cdots = P_U = P$ and $\mathbf{A}_1 = \mathbf{A}_2 = \cdots = \mathbf{A}_U = \mathbf{A}$ in the ray-based channel model (1). Therefore, we omit the subscript u of P_u and $\mathbf{A}_u$ for the rest of this subsection. Since the ZF precoding vector $\check{\mathbf{v}}_i$ is the normalized i-th column of $\check{\mathbf{H}}^{\dagger} = \check{\mathbf{H}}(\check{\mathbf{H}}^{\mathrm{H}}\check{\mathbf{H}})^{-1}$, by combining (32), we can express the precoding vector as $\check{\mathbf{v}}_i = \mathbf{A}\mathbf{p}$ where $\|\mathbf{p}\| = 1$. Therefore we can upper bound the inter-user interference as

$$\begin{aligned} \mathrm{E}\left[\left|\mathbf{e}_{g,u}^{\mathrm{H}}\mathbf{A}_u^{\mathrm{H}}\check{\mathbf{v}}_i\right|^2\right] &\leq \mathrm{E}\left[\left|\mathbf{e}_{g,u}^{\mathrm{H}}\mathbf{A}^{\mathrm{H}}\mathbf{A}\mathbf{p}\right|^2\right] \\ &= \mathrm{E}\left[\mathbf{p}^{\mathrm{H}}\mathbf{A}^{\mathrm{H}}\mathbf{A}\mathrm{E}\left[\mathbf{e}_{g,u}\mathbf{e}_{g,u}^{\mathrm{H}}\right]\mathbf{A}^{\mathrm{H}}\mathbf{A}\mathbf{p}\right] \end{aligned} \quad (38)$$

By substituting $\mathbf{A}^{\mathrm{H}}\mathbf{A} \overset{M\to\infty}{=} \mathbf{I}_P$ and $\mathrm{E}\left[\mathbf{e}_{g,u}\mathbf{e}_{g,u}^{\mathrm{H}}\right] = \sigma_{e_{g,u}}^2\mathbf{I}_P$, we obtain the upper bound on the inter-user interference as

$$\mathrm{E}\left[\left|\mathbf{e}_{g,u}^{\mathrm{H}}\mathbf{A}_u^{\mathrm{H}}\check{\mathbf{v}}_i\right|^2\right] \leq \sigma_{e_{g,u}}^2. \quad (39)$$

By combining (37) and (39), we further obtain the upper bound on the rate gap of the proposed channel subspace based analog feedback technique as

$$\begin{aligned} \Delta R_{\text{Analog}} &\leq \log_2\left(1+\frac{\gamma(U-1)}{U}\sigma_{e_{g,u}}^2\right) \\ &= \log_2\left(1+\frac{\gamma(U-1)}{U}(1+\mu\gamma_{\mathrm{U}})^{-1}\right). \end{aligned} \quad (40)$$

C. Quantized Channel Feedback v.s. Analog Channel Feedback

Recall the rate gap $\Delta R_{\text{Quanized}}$ of the proposed quantized feedback technique using the AoD-adaptive subspace codebook in (29). We assume that the AoD information is perfectly known, thus $\beta = 0$. Similar to (12), we can easily obtain that $\mathrm{E}\left[\|\mathbf{h}\|^2\right] = P$. Therefore the rate gap $\Delta R_{\text{Quanized}}$ of the quantized channel feedback technique can be further bounded as

$$\Delta R_{\text{Quanized}} \leq \log_2\left(1+\frac{\gamma P(U-1)}{U(P-1)}2^{-\frac{B}{P-1}}\right). \quad (41)$$

Following the assumption in [31] that the digital feedback link can be operated error-free and at capacity, i.e., $\log_2(1+\gamma_{\mathrm{U}})$ bits can be transmitted per channel use. To feedback the path gain vector $\mathbf{g}$ in our proposed channel subspace based analog feedback technique, μP channel uses are required where μ is the number of channel use per element. Therefore, $B = \mu P\log_2(1+\gamma_{\mathrm{U}})$ bits can be transmitted using the same feedback resource as the analog channel feedback. By substituting $B = \mu P\log_2(1+\gamma_{\mathrm{U}})$ into (41), we rewrite the rate gap $\Delta R_{\text{Quanized}}$ of the proposed quantized feedback technique using the AoD-adaptive subspace codebook as

$$\Delta R_{\text{Quanized}} \leq \log_2\left(1+\frac{\gamma P(U-1)}{U(P-1)}(1+\gamma_{\mathrm{U}})^{-\frac{\mu P}{P-1}}\right). \quad (42)$$

Remark 2: We compare the rate gap of the analog and quantized feedback technique as the scale factor α grows large with a constant uplink SNR γ_{U}. For the analog feedback technique (40), $2^{\Delta R_{\text{Analog}}}$ decreases inversely with the scale factor μ when $\mu \to \infty$. While for the quantized channel feedback technique (42), $2^{\Delta R_{\text{Quanized}}}$ decreases exponentially with the scale factor μ when $\mu \to \infty$. Therefore, we can conclude that the quantized feedback technique outperforms the analog feedback technique when μ grows large, which will be verified by simulations.

Remark 3: We compare the rate gap of the analog and quantized feedback technique as the uplink SNR γ_{U} grows large with a constant scale factor μ. For the analog feedback technique (40), $2^{\Delta R_{\text{Analog}}}$ decreases inversely with the uplink SNR γ_{U} when $\gamma_{\mathrm{U}} \to \infty$. For the quantized feedback technique (42), $2^{\Delta R_{\text{Quanized}}}$ decreases proportionally with $\frac{\mu P}{P-1}$-power of γ_{U} when $\gamma_{\mathrm{U}} \to \infty$. Therefore, we should consider two cases: $\mu < \frac{P-1}{P}$ and $\mu > \frac{P-1}{P}$. If $\mu < \frac{P-1}{P}$, the analog feedback technique outperforms the quantized feedback technique when the uplink SNR grows large. If $\mu > \frac{P-1}{P}$, the quantized feedback technique outperforms the analog channel feedback technique when the uplink SNR grows large.

TABLE I

SYSTEM PARAMETERS FOR SIMULATIONS

The number of BS antennas M	$8 \sim 200$
The number of users U	6
The number of dominant paths per user P	$1 \sim 5$
The path AoD ϕ	$\mathcal{U}[-\frac{1}{2}\pi, \frac{1}{2}\pi]$
The downlink receiver SNR in (30)	$1 \sim 10$ dB
The number of AoD quantization bits B_0	$2 \sim 9$

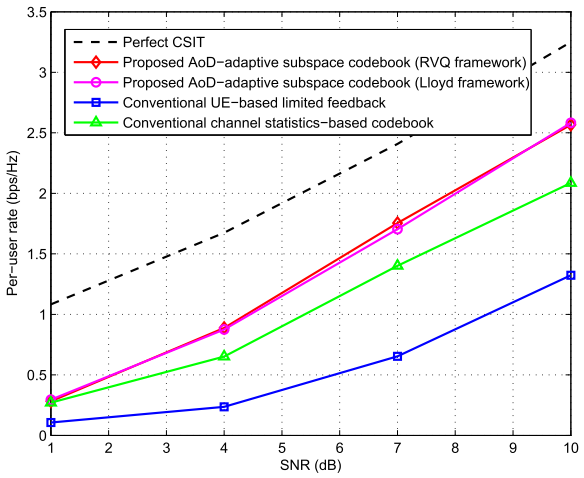

Fig. 3. The per-user rate of the ideal case of the perfect CSIT and the practical case of quantized feedback techniques, where the proposed AoD-adaptive subspace codebook under the RVQ framework and the Lloyd framework, the traditional channel statistics-based codebook [15], and the traditional UE-based limited feedback method [9] are considered. The rate gap between the ideal case of the perfect CSIT and the proposed codebook is limited within a constant value when the receiver SNR increases, which is consistent with our theoretical analysis in Section IV-C.

Note that our comparison is based on the proposed channel subspace based analog feedback technique and the proposed quantized feedback technique using the AoD-adaptive subspace codebook. Our analytical results are consistent with the comparison results between the traditional analog feedback technique and the traditional quantized feedback technique using the RVQ codebook [31].

VI. SIMULATION RESULTS

A simulation study is carried out in this section. The main system parameters are described in Table I. We consider the ULA of antennas at the BS with the array response $\mathbf{a}(\phi_{u,i})$ in (2). The per-user rate R_{Ideal} of the ideal case of the perfect CSIT is calculated according to (13). The per-user rate $R_{\text{Quantized}}$ of the practical case of the proposed quantized feedback technique using the AoD-adaptive subspace codebook is calculated according to (9). The per-user rate R_{Analog} of the practical case of the proposed channel subspace based analog feedback technique is calculated according to (35). The proposed AoD-adaptive subspace codebook is generated under the RVQ framework except for Fig. 3, where both the RVQ framework and Lloyd framework are considered. The downlink receiver SNR is 10 dB for all figures except for Fig. 3. The number of BS antennas is $M = 128$ for all figures except for Fig. 4. The number of dominant paths per user is $P = 4$ for all figures except for Fig. 6.

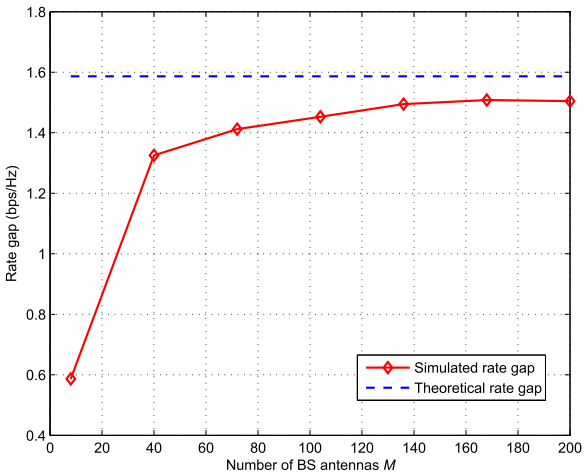

Fig. 4. Comparison between the theoretical upper bound (29) on the rate gap and the simulated rate gap of the proposed AoD-adaptive subspace codebook against the number of BS antennas M. The theoretical rate gap becomes tight enough when the number of BS antennas exceeds 120.

Fig. 3 shows the per-user rate of the ideal case of the perfect CSIT and the practical case of the quantized feedback techniques. For the quantized feedback techniques, the proposed AoD-adaptive subspace codebook under the RVQ framework and the Lloyd framework, the traditional channel statistics-based codebooks [15], and the traditional UE-based limited feedback method [9] are considered. The number of AoD quantization bits is $B_0 = 7$ and the number of feedback bits B is set as (30) with $b = 3$. We observe that the rate gap between the ideal case of the perfect CSIT and the proposed AoD-adaptive subspace codebook can be limited within a constant value when the receiver SNR increases, which is consistent with our theoretical analysis in Section IV-C. The proposed codebook under the RVQ framework and the Lloyd framework have similar performance. Besides, the proposed codebook outperforms the traditional channel statistics-based codebook and the UE-based limited feedback method.

Then, we evaluate the analytical upper bound (29) on the rate gap of the proposed AoD-adaptive subspace codebook against the number of BS antennas M. The number of feedback bits B is set as (30) with $b = 3$. We assume that the AoD information is perfectly known for the proposed codebook. Fig. 4 shows the theoretical upper bound on rate gap (29) and the simulated rate gap of the proposed codebook, which is obtain by $R_{\text{Quantized}} - R_{\text{Ideal}}$. We observe that the theoretical rate gap becomes tight when the number of BS antennas exceeds 120.

Fig. 5 shows the required number of feedback bits B for the proposed AoD-adaptive subspace codebook to limit the rate gap $\Delta R_{\text{Quanized}} = R_{\text{Ideal}} - R_{\text{Quantized}}$ within $\log_2 b = \log_2 2 = 1$ bps/Hz against the number of dominant paths per user P. The number of feedback bits B is set as (30) with $b = 2$ and the AoD information is assumed to be perfectly known for the proposed codebook. We observe that the required number of feedback bits B scales linearly with the number of dominant paths P. It is consistent with the theoretical result (30) on the required number of feedback bits, which is also shown in Fig. 5 for comparison. Note that the required number of

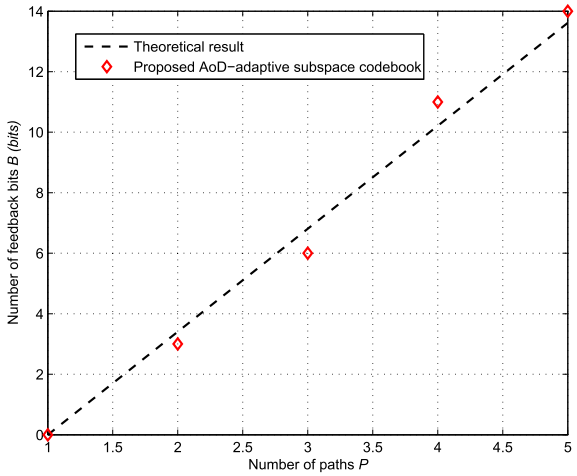

Fig. 5. The required number of feedback bits B for the proposed AoD-adaptive subspace codebook to limit the rate gap within a constant value. B scales linearly with the number of dominant paths per user P, which is consistent with the theoretical result (30) on the required number of feedback bits.

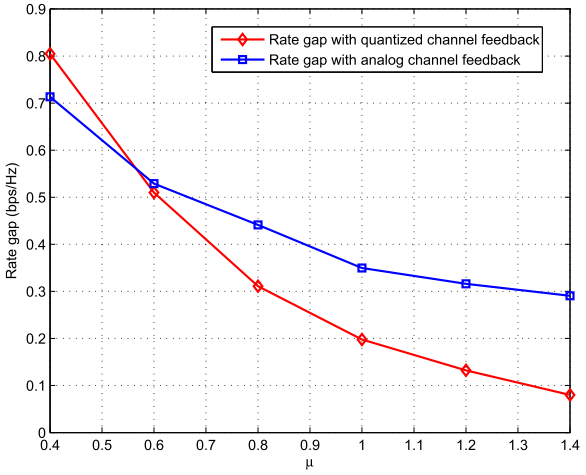

Fig. 7. The rate gap comparison between the proposed quantized feedback technique using the AoD-adaptive subspace codebook $\Delta R_{\text{Quanized}}$ and the proposed channel subspace based analog feedback technique ΔR_{Analog}. The rate gap of the quantized feedback technique decreases (exponentially) more quickly than that of the analog feedback technique (inversely).

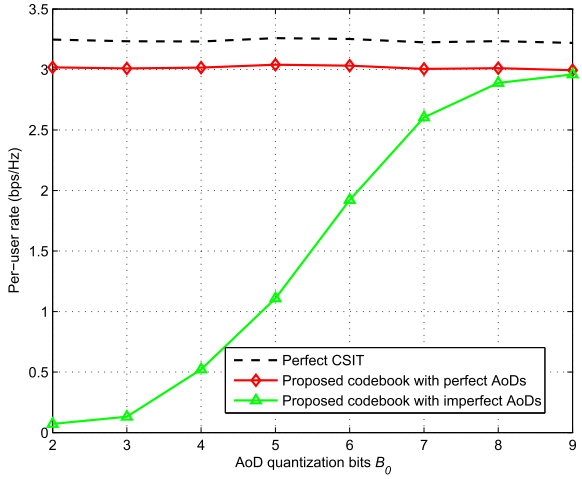

Fig. 6. The per-user rate of the proposed AoD-adaptive subspace codebook against the number of AoD quantization bits B_0. The per-user rate of the proposed codebook increases with B_0. Since the angle coherence time is comparably long, the average required number of AoD quantization bits is not large.

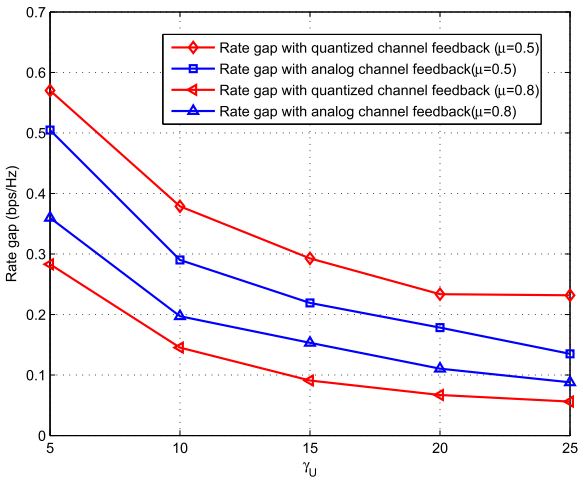

Fig. 8. The rate gap comparison between the proposed quantized feedback technique using the AoD-adaptive subspace codebook $\Delta R_{\text{Quanized}}$ and the proposed channel subspace based analog feedback technique ΔR_{Analog}. $\mu = 0.5 \leq \frac{P-1}{P}$ and $\mu = 0.8 \geq \frac{P-1}{P}$ are configured, respectively. The simulated results are consistent with the **Remark 3** in section V.

feedback bits $B = 0$ when $P = 1$. This is because no feedback bit is required for the LOS channel ($P = 1$) when the AoD information is known.

In Fig. 6, we compare the per-user rate of the proposed AoD-adaptive subspace codebook with the perfect AoD information and the imperfect AoD information. For the imperfect AoD information case, each AoD is quantized by B_0 bits. The number of feedback bits B is set as (30) with $b = 3$. We observe that the per-user rate of the proposed AoD-adaptive subspace codebook increases with the number of AoD quantization bits B_0. Note that when $B_0 = 8$, the per-user rate of the proposed AoD-adaptive subspace codebook with imperfect AoDs is close to that with perfect AoDs. Since the angle coherence time is comparably long, the average required number of AoD quantization bits is not large. For example, assuming the angle coherence time is 10 times of the channel coherence time, the average number of AoD quantization bits is $P \times B_0/10 \approx 3$.

Finally, we compare the rate gap of proposed quantized feedback technique using the AoD-adaptive subspace codebook and the proposed channel subspace based analog feedback technique in Fig. 7 and Fig. 8. The number of feedback bits is set as $B = \mu P \log_2(1 + \gamma_{\text{U}})$ and the AoD information is assumed to be perfectly known. As shown in Fig. 7, where a constant uplink SNR $\gamma_{\text{U}} = 5$ is configured, the rate gap of the quantized feedback technique decreases (exponentially) faster than that of the analog feedback technique (inversely) as μ increase. That is to say, the quantized feedback technique outperforms the analog feedback technique when μ grows large, which is consistent with the **Remark 2**. As shown

in Fig. 8, the rate gap of the quantized feedback technique is larger than that of the analog feedback technique when $\mu = 0.5 \leq \frac{P-1}{P}$ is configured. While the rate gap of the quantized feedback technique is smaller than that of the analog feedback technique when $\mu = 0.8 \geq \frac{P-1}{P}$ is configured. These simulated results are consistent with the **Remark 3**.

VII. Conclusions

In this paper, we have proposed the AoD-adaptive subspace codebook for channel feedback in FDD massive MIMO systems. By exploiting the property that path AoDs vary more slowly than path gains, the proposed codebook can achieve significant reduction of feedback overhead. We have also provided performance analysis of the proposed codebook in the large-dimension regime, from which we have shown that the required number of feedback bits only scales linearly with the number of dominant paths, not with the number of BS antennas. Moreover, we have compared the proposed quantized feedback technique using the AoD-adaptive codebook with a proposed channel subspace based analog feedback technique. These analytical results are verified by extensive simulations.

Appendix I

In this Apppendix, we prove the following Lemma 3 in the large-dimension regime which is used in the proof of Lemma 2 as well as in the analysis of quantization error in Section IV-B.

Lemma 3: The steering vectors of the dominant paths with distinguished AoDs (i.e., the column vectors of $\mathbf{A}$) are asymptotically orthogonal to each other when $M \to \infty$, i.e., $\mathbf{A}^{\mathrm{H}}\mathbf{A} \overset{M\to\infty}{=} \mathbf{I}_P$. When the AoD quantization error is small, $\mathbf{A}^{\mathrm{H}}\hat{\mathbf{A}} \overset{M\to\infty}{=} \mathcal{K}\mathbf{I}_P$ where $|\mathcal{K}|^2 \geq 1 - \frac{M^2}{3}(\pi\frac{d}{\lambda})^2 r^2 2^{-2B_0}$.

Proof: For the scenario with a ULA of antennas at the BS, the (p,q)-th element of $\mathbf{A}^{\mathrm{H}}\hat{\mathbf{A}}$ can be expressed as

$$\left|\mathbf{a}(\phi_p)^{\mathrm{H}}\mathbf{a}(\hat{\phi}_q)\right| = \left|\Upsilon\left(\frac{d}{\lambda}\delta_{p,q}\right)\right|, \tag{43}$$

where $\delta_{p,q} = \sin(\phi_p) - \sin(\hat{\phi}_q)$ and $\Upsilon(x) \triangleq \frac{\sin(M\pi x)}{M\sin(\pi x)}$. According to the characteristics of $\Upsilon(x)$, when $|x| \gg \frac{1}{M}$, i.e., $|\delta_{p,q}| \gg \frac{\lambda}{Md}$, we have $|\Upsilon(x)| \overset{M\to\infty}{=} 0$ [32]. Now we consider the following two cases:

i) If $\hat{\mathbf{A}} = \mathbf{A}$, i.e., $\delta_{p,q} = \sin\phi_p - \sin\phi_q$, the absolute diagonal element of $\mathbf{A}^{\mathrm{H}}\mathbf{A}$ can be expressed as $\left|\mathbf{a}(\phi_p)^{\mathrm{H}}\mathbf{a}(\phi_p)\right| = \left|\Upsilon\left(\frac{d}{\lambda}\delta_{p,p}\right)\right| = |\Upsilon(0)| = 1$. For the non-diagonal element $\mathbf{a}(\phi_p)^{\mathrm{H}}\mathbf{a}(\phi_q)$ $(p \neq q)$, since AoDs ϕ_p and ϕ_q are distinguished enough, i.e., $|\delta_{p,q}| = |\sin\phi_p - \sin\phi_q| \gg \frac{\lambda}{Md}$, the absolute non-diagonal element of $\mathbf{A}^{\mathrm{H}}\mathbf{A}$ can be expressed as $\left|\mathbf{a}(\phi_p)^{\mathrm{H}}\mathbf{a}(\phi_q)\right| = \left|\Upsilon\left(\frac{d}{\lambda}\delta_{p,q}\right)\right| \overset{M\to\infty}{=} 0$. Therefore, we have $\mathbf{A}^{\mathrm{H}}\mathbf{A} \overset{M\to\infty}{=} \mathbf{I}_P$.

ii) Otherwise $\hat{\mathbf{A}} \neq \mathbf{A}$, i.e., $\delta_{p,q} = \sin\phi_p - \sin\hat{\phi}_q$, the absolute diagonal element of $\mathbf{A}^{\mathrm{H}}\hat{\mathbf{A}}$ can be expressed as $\left|\mathbf{a}(\phi_p)\mathbf{a}\left(\hat{\phi}_p\right)^{\mathrm{H}}\right| = \left|\Upsilon\left(\frac{d}{\lambda}\delta_{p,p}\right)\right|$, where $|\delta_{p,p}| = \left|\sin\phi_p - \sin\hat{\phi}_p\right|$ is the AoD quantization error. With uniform quantization, $|\delta_{p,p}| \leq r2^{-B_0}$, where r is the difference between the maximum and minimum values over which $\sin(\phi_p)$ is quantized and B_0 is the number of AoD quantization bits. We denote the diagonal element of $\mathbf{A}^{\mathrm{H}}\hat{\mathbf{A}}$ as $\mathcal{K} = \mathbf{a}(\phi_p)^{\mathrm{H}}\mathbf{a}\left(\hat{\phi}_p\right)$. By using (43), we have

$$\begin{aligned}|\mathcal{K}|^2 &= \frac{\sin^2\left(\pi\frac{d}{\lambda}\delta_{p,p}M\right)}{M^2\sin^2\left(\pi\frac{d}{\lambda}\delta_{p,p}\right)} \\ &\overset{(a)}{\approx} 1 - \frac{M^2}{3}\left(\pi\frac{d}{\lambda}\right)^2\delta_{p,p}^2 \\ &\overset{(b)}{\geq} 1 - \frac{M^2}{3}\left(\pi\frac{d}{\lambda}\right)^2 r^2 2^{-2B_0},\end{aligned} \tag{44}$$

where (a) is obtained by the second-order Taylor's expansion of $\sin^2\left(\pi\frac{d}{\lambda}\delta_{p,p}M\right) = \left(\pi\frac{d}{\lambda}\delta_{p,p}M\right)^2 - \left(\pi\frac{d}{\lambda}\delta_{p,p}M\right)^4/3$ and the first-order Taylor's expansion of $\sin^2\left(\pi\frac{d}{\lambda}\delta_{p,p}\right) = \left(\pi\frac{d}{\lambda}\delta_{p,p}\right)^2$. (b) holds true due to $|\delta_{p,p}| \leq r2^{-B_0}$. For the non-diagonal element $\mathbf{a}(\phi_p)^{\mathrm{H}}\mathbf{a}\left(\hat{\phi}_q\right)$ $(p \neq q)$, we have

$$\begin{aligned}|\delta_{p,q}| &= |\sin\phi_p - \sin\hat{\phi}_q| \\ &= |\sin\phi_p - \sin\phi_q + \sin\phi_q - \sin\hat{\phi}_q| \\ &\geq |\sin\phi_p - \sin\phi_q| - |\sin\phi_q - \sin\hat{\phi}_q| \\ &\overset{(a)}{\geq} |\sin\phi_p - \sin\phi_q| - r2^{-B_0},\end{aligned} \tag{45}$$

where (a) is true since the AoD quantization $|\sin\phi_q - \sin\hat{\phi}_q| \leq r2^{-B_0}$. We assume that B_0 is properly chosen (large enough) so that $|\delta_{p,q}| \gg \frac{\lambda}{dM}$. Thus, the absolute non-diagonal element of $\mathbf{A}^{\mathrm{H}}\hat{\mathbf{A}}$ can be expressed as $\left|\mathbf{a}(\phi_p)^{\mathrm{H}}\mathbf{a}\left(\hat{\phi}_q\right)\right| = \left|\Upsilon\left(\frac{d}{\lambda}\delta_{p,q}\right)\right| \overset{M\to\infty}{=} 0$. Therefore, we have proved that $\mathbf{A}^{\mathrm{H}}\hat{\mathbf{A}} \overset{M\to\infty}{=} \mathcal{K}\mathbf{I}_P$.

In summary, for the scenario of a ULA of antennas at the BS, $\mathbf{A}^{\mathrm{H}}\mathbf{A} \overset{M\to\infty}{=} \mathbf{I}_P$ and $\mathbf{A}^{\mathrm{H}}\hat{\mathbf{A}} \overset{M\to\infty}{=} \mathcal{K}\mathbf{I}_P$, where $|\mathcal{K}|^2 \geq 1 - \frac{M^2}{3}(\pi\frac{d}{\lambda})^2 r^2 2^{-2B_0}$.

For the scenario of a UPA of antennas at the BS, we can rewrite the antenna array response (3) as

$$\mathbf{a}(\phi,\theta) = \mathbf{a}_h(\phi,\theta) \otimes \mathbf{a}_v(\phi,\theta), \tag{46}$$

where the horizontal steering vector is $\mathbf{a}_h(\phi,\theta) = \frac{1}{\sqrt{M_1}}\left[1, e^{j2\pi\frac{d}{\lambda}\cos\theta\sin\phi}, \cdots, e^{j2\pi\frac{d}{\lambda}(M_1-1)\cos\theta\sin\phi}\right]^{\mathrm{T}}$ and the vertical steering vector is $\mathbf{a}_v(\phi,\theta) = \frac{1}{\sqrt{M_2}}\left[1, e^{j2\pi\frac{d}{\lambda}\sin\theta}, \cdots, e^{j2\pi\frac{d}{\lambda}(M_2-1)\sin\theta}\right]^{\mathrm{T}}$. Similar to the ULA scenario, we calculate the (p,q)-th element of $\mathbf{A}^{\mathrm{H}}\hat{\mathbf{A}}$ as

$$\begin{aligned}\mathbf{a}(\phi_p,\theta_p)^{\mathrm{H}}\mathbf{a}\left(\hat{\phi}_q,\hat{\theta}_q\right) &= \left(\mathbf{a}_h(\phi_p,\theta_p)^{\mathrm{H}}\mathbf{a}_h(\hat{\phi}_q,\hat{\theta}_q)\right) \\ &\otimes \left(\mathbf{a}_v(\phi_p,\theta_p)^{\mathrm{H}}\mathbf{a}_v(\hat{\phi}_q,\hat{\theta}_q)\right).\end{aligned} \tag{47}$$

By denoting $\zeta_{p,q} = \cos\theta_p\sin\phi_p - \cos\hat{\theta}_q\sin\hat{\phi}_q$ and $\xi_{p,q} = \sin\theta_p - \sin\hat{\theta}_q$, we have

$$\left|\mathbf{a}(\phi_p,\theta_p)^{\mathrm{H}}\mathbf{a}\left(\hat{\phi}_q,\hat{\theta}_q\right)\right| = \left|\Upsilon\left(\frac{d}{\lambda}\zeta_{p,q}\right)\right|\left|\Upsilon\left(\frac{d}{\lambda}\xi_{p,q}\right)\right|. \tag{48}$$

Now we consider the following two cases:

i) If $\hat{\mathbf{A}} = \mathbf{A}$, i.e., $\zeta_{p,q} = \cos\theta_p \sin\phi_p - \cos\theta_q \sin\phi_q$ and $\xi_{p,q} = \sin\theta_p - \sin\theta_q$, the absolute diagonal element of $\mathbf{A}^{\mathrm{H}}\mathbf{A}$ can be expressed as $\left|\mathbf{a}\left(\phi_p,\theta_p\right)^{\mathrm{H}}\mathbf{a}\left(\phi_p,\theta_p\right)\right| = \left|\Upsilon\left(\frac{d}{\lambda}\zeta_{p,p}\right)\right|\left|\Upsilon(\frac{d}{\lambda}\xi_{p,p})\right| = |\Upsilon(0)||\Upsilon(0)| = 1$. The absolute non-diagonal element of $\mathbf{A}^{\mathrm{H}}\mathbf{A}$ is $\left|\mathbf{a}\left(\phi_p,\theta_p\right)^{\mathrm{H}}\mathbf{a}\left(\phi_q,\theta_q\right)\right| = \left|\Upsilon\left(\frac{d}{\lambda}\zeta_{p,q}\right)\right|\left|\Upsilon\left(\frac{d}{\lambda}\xi_{p,q}\right)\right| \overset{M\to\infty}{=} 0$, since the azimuth AoDs ϕ_p and ϕ_q (elevation AoDs θ_p and θ_q) are distinguished enough. Therefore, we have $\mathbf{A}^{\mathrm{H}}\mathbf{A} \overset{M\to\infty}{=} \mathbf{I}_P$.

ii) Otherwise $\hat{\mathbf{A}} \neq \mathbf{A}$, i.e., $\zeta_{p,q} = \cos\theta_p \sin\phi_p - \cos\hat{\theta}_q \sin\hat{\phi}_q$ and $\xi_{p,q} = \sin\theta_p - \sin\hat{\theta}_q$. For the diagonal element, we have

$$\begin{aligned}|\mathcal{K}|^2 &= \left|\Upsilon\left(\frac{d}{\lambda}\zeta_{p,p}\right)\right|^2\left|\Upsilon\left(\frac{d}{\lambda}\xi_{p,p}\right)\right|^2 \\ &= \frac{\sin^2\left(\pi\frac{d}{\lambda}\zeta_{p,p}M_1\right)}{M_1^2\sin^2\left(\pi\frac{d}{\lambda}\zeta_{p,p}\right)} \times \frac{\sin^2\left(\pi\frac{d}{\lambda}\xi_{p,p}M_2\right)}{M_2^2\sin^2\left(\pi\frac{d}{\lambda}\xi_{p,p}\right)}. \quad (49)\end{aligned}$$

For the non-diagonal element, similar to the ULA scenario, when the number of AoD quantization bits B_0 is properly chosen, we have $\left|\mathbf{a}\left(\phi_p,\theta_p\right)^{\mathrm{H}}\mathbf{a}\left(\hat{\phi}_q,\hat{\theta}_q\right)\right| = \left|\Upsilon\left(\frac{d}{\lambda}\zeta_{p,q}\right)\right|\left|\Upsilon\left(\frac{d}{\lambda}\delta_{p,q}\right)\right| \overset{M\to\infty}{=} 0$. Therefore, we have $\mathbf{A}^{\mathrm{H}}\hat{\mathbf{A}} \overset{M\to\infty}{=} \mathcal{K}\mathbf{I}_P$.

In summary, for the scenario of a UPA of antennas at the BS, we have proved that $\mathbf{A}^{\mathrm{H}}\mathbf{A} \overset{M\to\infty}{=} \mathbf{I}_P$, and $\mathbf{A}^{\mathrm{H}}\hat{\mathbf{A}} \overset{M\to\infty}{=} \mathcal{K}\mathbf{I}_P$. ■

APPENDIX II

In this appendix, we prove the following Lemma 4 which is used in the proof of Lemma 2.

Lemma 4: In the extreme case that all U users share the same clusters around the BS, i.e., $P_1 = P_2 = , \cdots , = P_U = P$ and $\mathbf{A}_1 = \mathbf{A}_2 = , \cdots , = \mathbf{A}_U = \mathbf{A}$, the subscript u of P_u, $\mathbf{A}_u$ and $\hat{\mathbf{A}}_u$ can be omitted. We have $\mathrm{E}\left[|\mathbf{t}^{\mathrm{H}}\mathbf{u}|^2\right] = \frac{1}{P-1}$.

Proof: Based on Section IV, we know that $\mathbf{q} = \mathbf{A}\mathbf{t}$ and the feedback channel vector can be expressed as $\hat{\mathbf{h}}_u = \|\mathbf{h}_u\|\hat{\mathbf{A}}\mathbf{w}_{i_u}$. Considering that $\mathbf{q}$ is distributed in the null space of $\hat{\mathbf{h}}_u$ as shown in Lemma 2, we have

$$\mathbf{q}^{\mathrm{H}}\hat{\mathbf{h}}_u = \mathbf{t}^{\mathrm{H}}\mathbf{A}^{\mathrm{H}}\|\mathbf{h}_u\|\hat{\mathbf{A}}\mathbf{w}_{i_u} = 0, \quad (50)$$

where $\mathbf{A}^{\mathrm{H}}\hat{\mathbf{A}} \overset{M\to\infty}{=} \mathcal{K}\mathbf{I}_P$ according to Appendix I. Therefore, we have $\mathbf{t}^{\mathrm{H}}\mathbf{w}_{i_u} = 0$, i.e., $\mathbf{t}$ is isotropically distributed in the null space of $\mathbf{w}_{i_u}$.

On the other hand, based on Section IV, the ZF precoding vector can be expressed as $\hat{\mathbf{v}}_i = \mathbf{A}\mathbf{u}$, and the feedback channel vector can be expressed as $\hat{\mathbf{h}}_u = \|\mathbf{h}_u\|\hat{\mathbf{A}}\mathbf{w}_{i_u}$. Since the ZF precoding vector $\hat{\mathbf{v}}_i$ is orthogonal to $\hat{\mathbf{h}}_u$, i.e.,

$$\hat{\mathbf{v}}_i^{\mathrm{H}}\hat{\mathbf{h}}_u = \mathbf{u}^{\mathrm{H}}\mathbf{A}^{\mathrm{H}}\|\mathbf{h}_u\|\hat{\mathbf{A}}\mathbf{w}_{i_u} = 0, \quad (51)$$

where $\mathbf{A}^{\mathrm{H}}\hat{\mathbf{A}} \overset{M\to\infty}{=} \mathcal{K}\mathbf{I}_P$ according to Appendix I. Therefore, we have $\mathbf{u}^{\mathrm{H}}\mathbf{w}_{i_u} = 0$, i.e., $\mathbf{u}$ is isotropically distributed in the null space of $\mathbf{w}_{i_u}$.

Now we have proved that both $\mathbf{t}$ and $\mathbf{u}$ are unit-norm isotropic vectors in the null space of $\mathbf{w}_{i_u}$. Based on [5], we have

$$\mathrm{E}\left[|\mathbf{t}^{\mathrm{H}}\mathbf{u}|^2\right] = \frac{1}{P-1}. \quad (52)$$

■

REFERENCES

[1] W. Shen, L. Dai, G. Gui, Z. Wang, R. W. Heath, Jr., and F. Adachi, "AoD-adaptive subspace codebook for channel feedback in FDD massive MIMO systems," in *Proc. IEEE Int. Conf. Commun. (ICC)*, May 2017, pp. 1–5.

[2] F. Rusek *et al.*, "Scaling up MIMO: Opportunities and challenges with very large arrays," *IEEE Signal Process. Mag.*, vol. 30, no. 1, pp. 40–60, Jan. 2013.

[3] D. J. Love, R. W. Heath, V. K. N. Lau, D. Gesbert, B. D. Rao, and M. Andrews, "An overview of limited feedback in wireless communication systems," *IEEE J. Sel. Areas Commun.*, vol. 26, no. 8, pp. 1341–1365, Oct. 2008.

[4] D. J. Love, R. W. Heath, and T. Strohmer, "Grassmannian beamforming for multiple-input multiple-output wireless systems," *IEEE Trans. Inf. Theory*, vol. 49, no. 10, pp. 2735–2747, Oct. 2003.

[5] N. Jindal, "MIMO broadcast channels with finite-rate feedback," *IEEE Trans. Inf. Theory*, vol. 52, no. 11, pp. 5045–5060, Nov. 2006.

[6] V. Va, J. Choi, and R. W. Heath, Jr., "The impact of beamwidth on temporal channel variation in vehicular channels and its implications," *IEEE Trans. Veh. Technol.*, vol. 66, no. 6, pp. 5014–5029, Jun. 2017.

[7] P. H. Kuo, H. T. Kung, and P. A. Ting, "Compressive sensing based channel feedback protocols for spatially-correlated massive antenna arrays," in *Proc. IEEE Wireless Commun. Netw. Conf. (WCNC)*, Apr. 2012, pp. 492–497.

[8] X. Rao and V. K. N. Lau, "Distributed compressive CSIT estimation and feedback for FDD multi-user massive MIMO systems," *IEEE Trans. Signal Process.*, vol. 62, no. 12, pp. 3261–3271, Jun. 2014.

[9] P. N. Alevizos, X. Fu, N. Sidiropoulos, Y. Ye, and A. Bletsas. (2018). "Limited feedback channel estimation in massive MIMO with non-uniform directional dictionaries." [Online]. Available: https://arxiv.org/abs/1712.10085

[10] B. Lee, J. Choi, J.-Y. Seol, D. J. Love, and B. Shim, "Antenna grouping based feedback compression for FDD-based massive MIMO systems," *IEEE Trans. Commun.*, vol. 63, no. 9, pp. 3261–3274, Sep. 2015.

[11] A. Adhikary, J. Nam, J.-Y. Ahn, and G. Caire, "Joint spatial division and multiplexing—The large-scale array regime," *IEEE Trans. Inf. Theory*, vol. 59, no. 10, pp. 6441–6463, Oct. 2013.

[12] M. S. Sim, J. Park, C.-B. Chae, and R. W. Heath, Jr., "Compressed channel feedback for correlated massive MIMO systems," *IEEE/KICS J. Commun. Netw.*, vol. 18, no. 1, pp. 95–104, Feb. 2016.

[13] J. Choi, Z. Chance, D. J. Love, and U. Madhow, "Noncoherent trellis coded quantization: A practical limited feedback technique for massive MIMO systems," *IEEE Trans. Commun.*, vol. 61, no. 12, pp. 5016–5029, Dec. 2013.

[14] N. Ravindran, N. Jindal, and H. C. Huang, "Beamforming with finite rate feedback for LOS MIMO downlink channels," in *Proc. IEEE Global Commun. Conf. (GLOBECOM)*, Nov. 2007, pp. 4200–4204.

[15] D. J. Love and R. W. Heath, "Limited feedback diversity techniques for correlated channels," *IEEE Trans. Veh. Technol.*, vol. 55, no. 2, pp. 718–722, Mar. 2006.

[16] B. Clerckx, G. Kim, and S. Kim, "MU-MIMO with channel statistics-based codebooks in spatially correlated channels," in *Proc. IEEE GLOBECOM*, Dec. 2008, pp. 1–5.

[17] W. Shen, L. Dai, Y. Zhang, J. Li, and Z. Wang, "On the performance of channel-statistics-based codebook for massive MIMO channel feedback," *IEEE Trans. Veh. Technol.*, vol. 66, no. 8, pp. 7553–7557, Aug. 2017.

[18] *Study on Channel Model for Frequencies From 0.5 to 100 GHz V14.2.0*, document TR 38.901, 3GPP, 2017.

[19] K. Venugopal, A. Alkhateeb, N. González-Prelcic, and R. W. Heath, Jr., "Channel estimation for hybrid architecture-based wideband millimeter wave systems," *IEEE J. Sel. Areas Commun.*, vol. 35, no. 9, pp. 1996–2009, Sep. 2017.

[20] D. Tse and P. Viswanath, *Fundamentals of Wireless Communication*. Cambridge, U.K.: Cambridge Univ. Press, 2005.

[21] A. Alkhateeb, O. El Ayach, G. Leus, and R. W. Heath, Jr., "Channel estimation and hybrid precoding for millimeter wave cellular systems," *IEEE J. Sel. Topics Signal Process.*, vol. 8, no. 5, pp. 831–846, Oct. 2014.

[22] W. Shen, L. Dai, Y. Shi, B. Shim, and Z. Wang, "Joint channel training and feedback for FDD massive MIMO systems," *IEEE Trans. Veh. Technol.*, vol. 65, no. 10, pp. 8762–8767, Oct. 2016.

[23] J. Choi, D. J. Love, and P. Bidigare, "Downlink training techniques for FDD massive MIMO systems: Open-loop and closed-loop training with memory," *IEEE J. Sel. Topics Signal Process.*, vol. 8, no. 5, pp. 802–814, Oct. 2014.

[24] T. S. Rappaport *et al.*, "Millimeter wave mobile communications for 5G cellular: It will work!" *IEEE Access*, vol. 1, pp. 335–349, 2013.
[25] D. J. Ryan, "Performance of RVQ limited feedback beamforming over correlated channels," in *Proc. IEEE Wireless Commun. Netw. Conf. (WCNC)*, Apr. 2010, pp. 1–6.
[26] A. Narula, M. J. Lopez, M. D. Trott, and G. W. Wornell, "Efficient use of side information in multiple-antenna data transmission over fading channels," *IEEE J. Sel. Areas Commun.*, vol. 16, no. 8, pp. 1423–1436, Oct. 1998.
[27] Y. Linde, A. Buzo, and R. M. Gray, "An algorithm for vector quantizer design," *IEEE Trans. Commun.*, vol. 28, no. 1, pp. 84–95, Jan. 1980.
[28] R. O. Schmidt, "Multiple emitter location and signal parameter estimation," *IEEE Trans. Antennas Propag.*, vol. AP-34, no. 3, pp. 276–280, Mar. 1986.
[29] T. L. Marzetta and B. M. Hochwald, "Fast transfer of channel state information in wireless systems," *IEEE Trans. Signal Process.*, vol. 54, no. 4, pp. 1268–1278, Apr. 2006.
[30] H. Shirani-Mehr and G. Caire, "Channel state feedback schemes for multiuser MIMO-OFDM downlink," *IEEE Trans. Commun.*, vol. 57, no. 9, pp. 2713–2723, Sep. 2009.
[31] G. Caire, N. Jindal, M. Kobayashi, and N. Ravindran, "Quantized vs. analog feedback for the MIMO broadcast channel: A comparison between zero-forcing based achievable rates," in *Proc. IEEE Int. Symp. Inf. Theory*, Jun. 2007, pp. 2046–2050.
[32] X. Gao, L. Dai, Z. Chen, Z. Wang, and Z. Zhang, "Near-optimal beam selection for beamspace mmWave massive MIMO systems," *IEEE Commun. Lett.*, vol. 20, no. 5, pp. 1054–1057, May 2016.

Wenqian Shen received the B.S. degree from Xi'an Jiaotong University, Shaanxi, China, in 2013, and the Ph.D. degree in electronic engineering from Tsinghua University, Beijing, China, in 2018. She is currently a Post-Doctoral Research Fellow with the School of Information and Electronics, Beijing Institute of Technology, Beijing. Her research interests include massive MIMO and mmWave communications. She has published several journal and conference papers in the IEEE TRANSACTIONS ON VEHICULAR TECHNOLOGY, the IEEE ICC, and so on. She has received the IEEE ICC 2017 Best Paper Award.

Linglong Dai received the B.S. degree from Zhejiang University in 2003, the M.S. degree (Hons.) from the China Academy of Telecommunications Technology in 2006, and the Ph.D. degree (Hons.) from Tsinghua University, Beijing, China, in 2011. From 2011 to 2013, he was a Post-Doctoral Research Fellow with the Department of Electronic Engineering, Tsinghua University, where he was an Assistant Professor from 2013 to 2016 and has been an Associate Professor since 2016. He co-authored the book *mmWave Massive MIMO: A Paradigm for 5G* (Academic Press, Elsevier, 2016). He has published over 60 IEEE journal papers and over 40 IEEE conference papers. He also holds 15 granted patents. His current research interests include massive MIMO, millimeter-wave communications, NOMA, sparse signal processing, and machine learning. He has received five IEEE Best Paper Awards at the IEEE ICC 2013, the IEEE ICC 2014, the IEEE ICC 2017, the IEEE VTC 2017-Fall, and the IEEE ICC 2018. He has also received the Tsinghua University Outstanding Ph.D. Graduate Award in 2011, the Beijing Excellent Doctoral Dissertation Award in 2012, the China National Excellent Doctoral Dissertation Nomination Award in 2013, the URSI Young Scientist Award in 2014, the IEEE TRANSACTIONS ON BROADCASTING Best Paper Award in 2015, the Second Prize of Science and Technology Award of the China Institute of Communications in 2016, the *Electronics Letters* Best Paper Award in 2016, the IEEE COMMUNICATIONS LETTERS Exemplary Editor Award in 2017, the National Natural Science Foundation of China for Outstanding Young Scholars in 2017, and the IEEE ComSoc Asia-Pacific Outstanding Young Researcher Award in 2017. He currently serves as an Editor of the IEEE TRANSACTIONS ON COMMUNICATIONS, the IEEE TRANSACTIONS ON VEHICULAR TECHNOLOGY, and the IEEE COMMUNICATIONS LETTERS. Particularly, he is dedicated to reproducible research and has made a large amount of simulation code publicly available.

Byonghyo Shim received the B.S. and M.S. degrees in control and instrumentation engineering from Seoul National University, South Korea, in 1995 and 1997, respectively, and the M.S. degree in mathematics and the Ph.D. degree in electrical and computer engineering from the University of Illinois at Urbana–Champaign, USA, in 2004 and 2005, respectively. From 1997 and 2000, he was with the Department of Electronics Engineering, Korean Air Force Academy, as an Officer (First Lieutenant) and an Academic Full-Time Instructor. From 2005 to 2007, he was with Qualcomm Inc., San Diego, CA, USA, as a Staff Engineer. From 2007 to 2014, he was with the School of Information and Communication, Korea University, Seoul, as an Associate Professor. Since 2014, he has been with the Seoul National University, where he is currently a Professor with the Department of Electrical and Computer Engineering. His research interests include wireless communications, statistical signal processing, compressed sensing, and machine learning. He is an elected member of the Signal Processing for Communications and Networking Technical Committee of the IEEE Signal Processing Society. He was a recipient of the M. E. Van Valkenburg Research Award from the ECE Department, University of Illinois, in 2005, the Hadong Young Engineer Award from IEIE in 2010, and the Irwin Jacobs Award from Qualcomm and KICS in 2016. He has served as an Associate Editor of the IEEE TRANSACTIONS ON SIGNAL PROCESSING, the IEEE TRANSACTIONS ON COMMUNICATIONS, the IEEE WIRELESS COMMUNICATIONS LETTERS, and the *Journal of Communications and Networks*, and a Guest Editor of the IEEE JOURNAL ON SELECTED AREAS IN COMMUNICATIONS.

Zhaocheng Wang received the B.S., M.S., and Ph.D. degrees from Tsinghua University in 1991, 1993, and 1996, respectively. From 1996 to 1997, he was a Post-Doctoral Fellow with Nanyang Technological University, Singapore. From 1997 to 1999, he was a Research Engineer/Senior Engineer with OKI Techno Centre Pte. Ltd., Singapore. From 1999 to 2009, he was a Senior Engineer/Principal Engineer with Sony Deutschland GmbH, Germany. Since 2009, he has been a Professor with the Department of Electronic Engineering, Tsinghua University, where he is currently the Director of the Broadband Communication Key Laboratory, Beijing National Research Center for Information Science and Technology.

His research interests include millimeter wave communications, optical wireless communications, and digital broadcasting. He holds 34 U.S./EU granted patents (23 of them as the first inventor) and published over 135 peer-reviewed international journal papers. He authored or co-authored two books, which have been selected by the IEEE Series on Digital and Mobile Communication (Wiley–IEEE Press).

Prof. Wang is a fellow of the Institution of Engineering and Technology. He received the ICC2013 Best Paper Award, the OECC2015 Best Student Paper Award, the 2016 IEEE Scott Helt Memorial Award, the 2016 National Award for Science and Technology Progress (First Prize), and the ICC2017 Best Paper Award. He was the technical program co-chair of many international conferences, including ICC and GlobeSIP. He was an Associate Editor of the IEEE TRANSACTIONS ON WIRELESS COMMUNICATIONS from 2011 to 2015 and an Associate Editor of the IEEE COMMUNICATIONS LETTERS from 2013 to 2016.

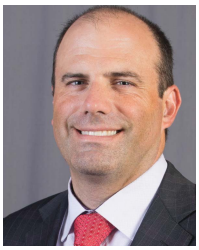

Robert W. Heath, Jr., received the B.S. and M.S. degrees in electrical engineering from the University of Virginia, Charlottesville, VA, USA, in 1996 and 1997, respectively, and the Ph.D. degree in electrical engineering from Stanford University, Stanford, CA, USA, in 2002. From 1998 to 2001, he was a Senior Member of the Technical Staff then as a Senior Consultant at Iospan Wireless Inc., San Jose, CA, USA, where he was involved in the design and implementation of the physical and link layers of the first commercial MIMO-OFDM communication system. Since 2002, he has been with the Department of Electrical and Computer Engineering, The University of Texas at Austin, where he is currently a Cullen Trust for Higher Education Endowed Professor and also a member of the Wireless Networking and Communications Group. He is also the President and the CEO of MIMO Wireless Inc. He has authored the book *Introduction to Wireless Digital Communication* (Prentice Hall, 2017) and *Digital Wireless Communication: Physical Layer Exploration Lab Using the NI USRP* (National Technology and Science Press, 2012) and co-authored the book *Millimeter Wave Wireless Communications* (Prentice Hall, 2014).

He is also an elected member of the Board of Governors for the IEEE Signal Processing Society, a licensed Amateur Radio Operator, a Private Pilot, and a registered Professional Engineer in Texas. He is a fellow of the National Academy of Inventors. He has been a co-author of 16 award winning conference and journal papers, including the 2010 and 2013 *EURASIP Journal on Wireless Communications and Networking* Best Paper Awards, the 2012 *IEEE Signal Processing Magazine* Best Paper Award, the 2013 Signal Processing Society Best Paper Award, the 2014 *EURASIP Journal on Advances in Signal Processing* Best Paper Award, the 2014 and 2017 *Journal of Communications and Networks* Best Paper Award, the 2016 IEEE Communications Society Fred W. Ellersick Prize, the 2016 IEEE Communications and Information Theory Societies Joint Paper Award, and the 2017 Marconi Prize Paper Award. He received the 2017 EURASIP Technical Achievement Award. He was a Distinguished Lecturer in the IEEE Signal Processing Society and is an ISI Highly Cited Researcher.